DUPLICATE ALSO (266)

# Long-Range Forecasting and Climate Research

## The Climate of the World

3. Climatic Forcing and Feedback Processes
I. Forcing from Above

4. Climatic Forcing and Feedback Processes
II. Interactions with the Land Surface

by

C. K. Folland and D. E. Parker

LRFC 23

July 1988

ORGS UKMO L

National Meteorological Library
FitzRoy Road, Exeter, Devon. EX1 3PB

FHIB

DUPLICATE ALSO

METEOROLOGICAL OFFICE
152711
15 AUG 1988
LIBRARY

LS/M013

LONG RANGE FORECASTING AND CLIMATE RESEARCH MEMORANDUM NO 23
(LRFC 23)

# THE CLIMATE OF THE WORLD

## 3. CLIMATIC FORCING AND FEEDBACK PROCESSES I. FORCING FROM ABOVE

## 4. CLIMATIC FORCING AND FEEDBACK PROCESSES II. INTERACTIONS WITH THE LAND SURFACE

by

C K FOLLAND AND D E PARKER

NOTES FOR TWO ADVANCED LECTURES FOR THE SCIENTIFIC OFFICERS' COURSE, METEOROLOGICAL OFFICE, 1988

Met O 13 (Synoptic Climatology Branch)
Meteorological Office
London Road
Bracknell
Berkshire
RG12 2SZ

July 1988

Note. This paper has not been published. permission to quote from it should be obtained from the Assistant Director (Synoptic Climatology), Meteorological Office.

LONDON, METEOROLOGICAL OFFICE.
Long-Range Forecasting and Climate Research
Memorandum No.23

The Climate of the world.
3. Climatic forcing and feedback processes. I.
Forcing from above.
4. Climatic forcing and feedback processes. II.
Interactions with the land surface.

00140988 FHIB

This Memorandum is the second in a series of seven on:

# THE CLIMATE OF THE WORLD

by

C K Folland and D E Parker

Based on ten Advanced Lectures for the Scientific Officers' Course, 1988, and one Advanced Lecture delivered by D J Carson in March 1982.

## INDEX TO SERIES


| | | |
|---|---|---|
| LRFC 22 | 1. | INTRODUCTION TO WORLD CLIMATE |
| | 2. | DESCRIPTION OF WORLD CLIMATE |
| LRFC 23 | 3. | CLIMATIC FORCING AND FEEDBACK PROCESSES. I. FORCING FROM ABOVE |
| | 4. | CLIMATIC FORCING AND FEEDBACK PROCESSES. II. INTERACTIONS WITH THE LAND SURFACE (Advanced Lectures 3 and 4). C K Folland and D E parker |
| LRFC 24 | 5. | OCEAN-ATMOSPHERE INTERACTION (Advanced Lecture 5). D E Parker and C K Folland |
| LRFC 25 | 6. | THE EL NINO/SOUTHERN OSCILLATION, THE QUASI-BIENNIAL OSCILLATION, AND THE 30-60 DAY VARIATIONS (Advanced Lecture 6. C K Folland and D E Parker |
| LRFC 26 | 7. | A REVIEW OF PALAEOCLIMATE FROM THE EARLY EARTH TO THE PLEISTOCENE ICE AGES |
| | 8. | CLIMATE FROM THE LATE GLACIAL TO THE "LITTLE ICE AGE" (Advanced Lectures 7 and 8) C K Folland and D E Parker |
| LRFC 27 | 9. | CLIMATIC CHANGE IN THE INSTRUMENTAL PERIOD (Advanced Lecture 9) D E Parker and C K Folland |
| LRFC 28 | 10. | CARBON DIOXIDE AND OTHER GREENHOUSE GASES, AND CLIMATIC VARIATION (WITH APPENDIX ON SIMPLE CLIMATE MODELS) (Advanced Lecture 10 plus an Advanced Lecture delivered by D J Carson in March 1982). D E Parker, C K Folland and D J Carson. |

ADVANCED LECTURE NO. 3

# CLIMATE FORCING AND FEEDBACK PROCESSES I - FORCING FROM ABOVE

C K FOLLAND AND D E PARKER

MET O 13

## SUMMARY

The Earth's climate is in principle sensitive to fluctuations of incoming solar radiation and also to changes in the extent to which outgoing radiation is re-absorbed by the atmosphere. First, changes in the total flux of energy from the sun are considered, followed by changes in the distribution with latitude and season of the solar radiation received by the Earth. The latter changes are known to have occurred on time-scales of $10^4$ to $10^6$ years in response to changes in the Earth's orbital configuration. The effects on outgoing radiation of carbon dioxide and other trace gases, and the effects of volcanic aerosols in the stratosphere, are subjected to basic mathematical treatment.

## 3.1 VARIATIONS IN SOLAR RADIATION AND CLIMATIC CHANGE

### 3.1.1 Introduction

Earth's climate is in principle sensitive to fluctuations of solar radiation if they persist for sufficient lengths of time. The average flux of energy from the sun at the mean distance of the earth is called the solar "constant" S and is about:-

$$S = 1370 \pm 15 \ Wm^{-2}$$

The average total flux of solar radiation received by the earth is, if R is the earth's radius:-

$$E_s = \pi R^2 S$$

because the Earth's profile from space is a disk of radius R.

The area of the earth's surface is $4\pi R^2$ so the average amount of energy per unit area received by the earth-atmosphere system is

$$S/4 = 342 \pm 4 \text{ Wm}^{-2}$$

It is easy to see that if the axis of rotation of the earth were normal to the plane intersecting the sun and all points in the earth's orbit, the incident energy per unit area would vary between a maximum (436 $\text{Wm}^{-2} = S/\pi$) at the equator and zero at the poles. However the tilt of the earth's rotation axis from this position is currently 23.44°. This results in large seasonal variations in radiation, though the simple calculation above is quite accurate close to the equator. Fig 3.1A shows the current zonally averaged radiation balance of the earth; the seasonal variations of insolation above the atmosphere are shown in Fig 3.1B. A fraction $\alpha = 0.3$ (approximately) of the radiation is reflected or scattered; this fraction is called the albedo. Figs 3.2 and 3.3 are a good guide to the surface albedo of the world with and without clouds.

The effective temperature of the earth is approximately given by

$$\sigma T_e^4 = (1-\alpha)S/4 \qquad (3.1)$$

Here we have assumed that the emissivity of the earth is one (not quite true), while $T_e$ is approximately the mass-weighted temperature of the atmosphere, subject to some modification by dynamical processes. The sensitivity of $T_e$ to S is shown by differentiating equation (3.1) and using

$$\Delta T_e = \frac{\partial T_e}{\partial S} \Delta S + \frac{\partial T_e}{\partial \alpha} \Delta\alpha \qquad (3.2)$$

If a 1% increase in S is accompanied by a 0.01 decrease in $\alpha$ due to the associated melting of snow and ice, or perhaps a reduction in low-level cloudiness, we obtain (using $T_e$ = -15°C = 258°K)

$\Delta T_e \simeq$ + 1.5°C/1% increase in S

If $\Delta\alpha = 0$ then $\Delta T_e$ is only +0.6°C/1% increase in S. So the sensitivity of the climate to S depends strongly on any associated changes in albedo. The ice/snow component of the feedback between solar radiation and climate is often called the ice-albedo feedback but its magnitude is uncertain. Nevertheless the climate system is very sensitive to long-lasting small changes in S.

### 3.1.2 Change of S

Does S actually change? Astronomers can say little about the fluctuations of S on short time scales but they believe it varies on geological time scales. Current theories suggest that S progressively increases as the sun gets older so that its value was perhaps 30% less 4 thousand million years ago than now. This question will be discussed in Lecture 7.

After compensation for the regular change of nearly 7% in radiation flux between January and July due to the fact that the earth currently moves in an elliptic orbit with eccentricity 0.0167, recent measurements from the solar Maximum Mission spacecraft do show small changes in S. Fig 3.4 (Hudson (1983)) shows rapid variations in S measured by an active cavity radiometer irradiance monitor (ACRIM) at a time of high solar activity, when many sunspots were sometimes visible on the solar disk. Although the mean absolute value of S shown in Fig. 3.4 (1368.2 $Wm^{-2}$) is in fact only accurate to about $\pm$ 0.5% ($\pm$ 7 $Wm^{-2}$) the relative changes in S are believed to be accurate to $\pm$ 0.1% (say $\pm$ 1 $Wm^{-2}$). The variations in Fig 3.4 approach four times this size and have a typical range of 0.2% over, say, a 10 day period. Reductions in S correspond to increased coverage of sunspots. Sunspots block the solar radiation at least temporarily, since the sunspot temperatures are typically about 4000°C rather than the normal

6000°C, and on daily and weekly time scales the warmer areas (faculae) sometimes surrounding sunspots apparently do not compensate. The radiation from the very small area covered by sunspots is reduced by a multiplying factor of $(4 / 6)^4$, about 0.2. These measurements were the first that indicated a real variation in the solar constant, though of course by very small amounts on short time scales. More recently, Willson and Hudson (1988) have shown that the total solar irradiance between 1980 and 1987 varied on interannual time scales in phase with the 11-year sunspot cycle (Fig 3.5), in contrast to the short-term variations in Fig 3.4 which were in antiphase with the coverage of sunspots. The short-period variations in 1980 in Fig 3.5 exceeded those after March 1984 because the sun was more active in 1980. However the short-term variability from late 1980 to March 1984 was enhanced by a fault in the satellite's stabilization, which was rectified by the space-shuttle astronauts in 1984. The 11-year sunspot cycle is also associated with in-phase fluctuation of the intensity of ultraviolet radiation (Donnelly (1983)). Because solar activity and the number of sunspots also vary on timescales of about 80 years and maybe on longer timescales ((Eddy 1983) : Fig 3.6), the findings of Willson and Hudson in Fig 3.5 may lend support to associations of widespread cooler climates with a lack of sunspots, as eg during the Maunder minimum of the 17th Century, shown in Fig 3.6, when sunspots may have been virtually absent and the "Little Ice Age" reached its climax (Lecture 8).

There is active debate about the reliability of measurements of the solar diameter in the 17th and 18th Centuries (Ribes et al (1987); Morrison et al (1988)). This debate is relevant because theories of solar dynamics relate the sun's luminosity to its diameter. Gilliland (1983) claimed to detect small changes in solar radius on a dominant time-scale of 76 years using measurements of uncertain homogeneity made by astronomers since the mid-nineteenth century. This kind of evidence has to be seriously considered until the time comes when accurate measurements of the solar constant made over many years are available.

### 3.1.3 Changes in the distribution of solar radiation on earth with the seasons

Changes in the seasonal distribution of radiation occur on long time scales because of fluctuations in the orbit of the earth. Assuming no intrinsic change in S, the changes in orbit are accompanied by very small annually averaged changes in S because the mean earth-sun distance changes only by small amounts. However seasonal values of radiation received at given latitudes on earth change much more. The fact that the earth's orbit has varied in a systematic way in the past was first calculated by Laplace (1798) using Newton's laws of motion and of gravity. The variations were calculated in great detail, with suggestions for their climatic consequences, by the Yugoslav mathematician Milutin Milankovitch (1941). Fig 3.7 shows the three basic types of orbital variation that occur, discussed in detail by Berger (1984):-

(a) The eccentricity of the earth's orbit changes on timescales close to $10^5$ years between values of about e = 0 and e = 0.06. The current value of e is 0.0167.

(b) The angle of tilt of the earth's spin axis ('the obliquity of the ecliptic') relative to the plane passing through all points on the earth's orbit (plane of the ecliptic) varies on a timescale close to $41 \times 10^3$ years. The angle would be zero if the earth were in an 'upright' position with its spin axis normal to the ecliptic. At present the angle, q, = 23.44°. It fluctuates with variable amplitude between limits of about 22° and 24.5° and is at present decreasing on average by about 0.01°/60 years.

(c) The time of year when the earth is closest (perihelion) and furthest (aphelion) from the sun varies on timescales in the range $19\text{-}23 \times 10^3$ years. These changes are called the 'precession of the equinoxes' and are often measured by an angle, $\theta$ between the position of the earth in its orbit at the time of the Northern Hemisphere autumn solstice and the position at perihelion. At present, the earth

is at perihelion on approximately Jan 3rd so this angle is now 102°. The date of perihelion becomes later as time progresses, i.e it will be January 5th in 100 years time.

Fig 3.8 shows the computed changes in seasonal radiation at different latitudes for the last $10^6$ years.Superimposed on these slow changes are much smaller, faster, changes in the geometry of the earth's orbit largely due to the orbit of Jupiter and variations in the moon's orbit which occur on timescales of decades to centuries (Fig 3.9) (Borisenkov et al (1983)).

Are these longer timescale (tens of thousands of years) radiation changes important? They are sufficient to alter the July radiation in the Northern Hemisphere through a range of at least 20% in most latitudes even though there is negligible change (0.2%) in the total mean annual radiation. (Least average radiation is received when the orbit is circular). An increase of summer radiation would warm the summer climate, balanced of course by a decrease in winter radiation which should tend to cool the winter climate and so increase the seasonal contrast. Changes in atmospheric circulation should result: eg the monsoons might tend to be more vigorous if summer radiation were more intense in the Northern Hemisphere and the ITCZ might move further north. At present summer radiation is relatively weak, though not especially so. Although the earth is furthest from the sun in July, e is fairly low. Thus the earth does not get as far away from the sun in Northern Hemisphere summer at present as it did in some previous epochs. However if radiation decreases in summer and winters are still cold enough, some areas which lose their snow in summer when summer radiation is high may retain it when summer radiation is low. Albedo will increase and amplify any cooling effect. In this way snow fields and ice sheets might grow, given other favourable circumstances.

A simple test calculation was carried out by Mason (1976) who showed that the deficiency of incident radiation in Northern Hemisphere summer between 83000 and 18000 years before present (BP) may have been just enough to balance the latent heat of fusion produced between those dates, when the Northern Hemisphere ice sheets are thought to have expanded to their maximum size. He also calculated that the excess of incident summer

radiation from 16000 BP to 6000 BP was just enough to provide the latent heat of fusion required to melt the amount of ice that is believed, from geological evidence, to have disappeared between these two dates (90% of the difference between the volume of ice-age ice and that which exists now). As Mason was at pains to point out, the calculation was over-simple because losses of radiation, and relevant feedbacks, were ignored, and thus on their own the radiation deficiencies and excesses seemed insufficient to guarantee the waxing and waning of the ice sheets. On the other hand, the variations in summer radiation were of the correct order of magnitude to make a substantial contribution, given other favourable "positive feedback" processes. So it is very important to identify these other processes. The precessional 'Milankovitch' radiation changes are not entirely negligible on millennial timescales; since the High Middle Ages (1200 AD) the flux of solar radiation incident on the atmosphere around the summer solstice at the North Pole has decreased by nearly 0.5%.

### 3.1.4 Energy balance models

The equilibrium sensitivity of earth's climate to changes in S can be studied in an instructive if preliminary way using simple 'energy balance' models. Appendix I, prepared by David Carson for the 1982 Advanced Lectures and attached to Lecture 10 of this series, discusses simple models and their approach to calculating the consequences of changes in S and in carbon dioxide or other greenhouse gases. The results of many of these calculations are thought-provoking even if they turn out to be somewhat misleading. Figure A10.13 of Appendix I shows that a reduction of S by a few per cent might cause the earth to become completely glaciated; a subsequent increase in S of at least 30% might be needed to melt the ice that has formed. These conclusions do indicate the potential sensitivity of climate to S in the presence of albedo feedback and the likely non-linearity of the response of the climate system.

In Lecture 7 we shall discuss the effects of the Milankovitch radiation variations in more detail and the hypothesis that they are the pace-makers of the ice-age - interglacial fluctuations that have occurred quite regularly over the last 2-3 million years.

## 3.2 CARBON DIOXIDE AND THE GREENHOUSE EFFECT

### 3.2.1 General discussion

Carbon dioxide is present in only small amounts in the atmosphere but is increasing by about 0.5% a year at present. The current concentration is about 350 parts per million by volume (ppmv). Carbon dioxide is important since it strongly absorbs long-wave radiation and re-emits it, so is radiatively very active in the climate system. The following discussion is only schematic and is oversimplified in many ways. It is adapted from Gill (1982) and applies to carbon dioxide, water vapour and other 'greenhouse' gases.

Consider a greenhouse formed by placing a horizontal thin sheet of glass above the ground (Fig 3.10). Let this glass be nearly transparent to solar radiation, absorbing only a small fraction s, but much less transparent to terrestial radiation. Suppose the glass and ground are initially cold. Let a downward flux, I, of solar radiation commence. Most of I will reach the ground; assuming the ground is a black body (ie has zero albedo), the ground will warm up to a temperature $T_g$ and emit long-wave radiation with a flux U given by Stefan's law:-

$$U = \sigma T_g^4 \qquad (3.3)$$

Now let a fraction e of U be absorbed by the glass. The glass will warm up and emit a flux of radiation B. Equilibrium is reached when on both sides of the glass the upward and downward fluxes of radiation are equal.

Thus

$$I = (1-e)\,U + B \qquad \text{above the glass} \qquad (3.4)$$

$$(1-s)\,I = U-B \qquad \text{below the glass} \qquad (3.5)$$

It is easy to show that

$$\sigma T_g^4 = I \left[ \frac{1 - s/2}{1 - e/2} \right] \qquad (3.6)$$

If s were zero and e were 1 then

$$\sigma T_g^4 = 2\,I \qquad \text{from (3.6)}$$

or $B = I$, so the flux received by the ground would be twice the solar flux, and $T_g$ would have increased by a factor $\Delta T_g = 2^{1/4} = 19\%$ compared with the case for $e = 0$. Now s is about 0.2 for present conditions and if this were true when $e = 1$ then $\Delta T_g = 16\%$. An increase in $T_g$ of 19% would correspond to a surface temperature rise of about 50°C above the condition where e=0, if the albedo was zero: as the average amount of energy incident per unit area of the earth's surface is about $I = 342\ Wm^{-2}$, and $\sigma = 5.7 \times 10^{-8}\ Wm^{-2}\ K^{-4}$, then $T_g = 278°K$ for $e = 0$ and $\delta T_g = 53°C$. In practice $T_g + \delta T_g$ would be considerably less than 331°K because $e < 1$ and importantly because of vertical atmospheric readjustments including the conversion of some of I to latent heat. These provide a 'radiative-convective' equilibrium in which the atmosphere above the ground takes up some of the extra heat initially absorbed at the surface.

Of course, the 'glass' is in reality distributed continuously in the vertical and water vapour is an important greenhouse gas which is very variable in concentration geographically (see Lecture 10). A point to note is that the addition of a greenhouse gas to the atmosphere does not necessarily leave the effective solar radiation received by the earth-atmosphere system unchanged if changes to the earth-atmosphere albedo also result. If we include the effect of the albedo $\alpha$ of the earth-atmosphere system and replace the net solar radiation received by the ground by $(1-s)(1-\alpha)I$ (ignoring $\alpha s^2$) and the net downward solar radiation above the glass by $I(1-\alpha(1-s)^2)$ we obtain approximately:-

$$\sigma T_g^4 = \frac{I\left[1-\left(\frac{s+2\alpha-3\alpha s}{2}\right)\right]}{1 - e/2} \qquad (3.7)$$

Here we arbitrarily attribute the albedo (due to ground and clouds) to the whole layer below the 'glass' so $T_g$ is not really the ground temperature. If $\alpha$ decreases as e increases, $\sigma T_g^4$ will increase at a faster rate. This could happen if snow and ice melted or low cloudiness decreased. Under present day conditions where nominally $T_g$ = 287°K, s=0.2 and $\alpha$ = 0.3, equation (3.7) gives approximately e = 0.8 for carbon dioxide, ozone, water vapour and other trace greenhouse gases together. Thus, schematically, at present $U = \sigma T_g^4 \simeq 1.1I$ which implies that the long-wave radiation B incident on the ground from the atmosphere above is about 0.6I since the absorbed solar radiation $U-B = (1-s)(1-\alpha) I \simeq 0.5I$ at the surface. Figure 3.11 summarises the current radiation balance of the earth-atmosphere system. This shows that the direct net loss of long-wave radiation from the surface contributes 0.2I to balancing U-B, the remaining 0.3I being first converted to sensible or latent heat in the lower atmosphere. The sensible heat is then lost as long-wave radiation immediately and the latent heat is lost likewise once precipitation has occurred.

Lecture 10 discusses the physical basis and evidence for the potential effects of carbon dioxide in the climate system in more detail and Lectures 7 and 8 indicate its possible role in past climatic changes.

## 3.3 VARIATIONS IN VOLCANIC DUST IN THE STRATOSPHERE

### 3.3.1 Introduction

From time to time huge volcanic eruptions of the explosive kind create world-wide veils of finely-divided dust causing optical effects such as a reddened sun or moon or halo effects around the sun like Bishop's rings. During such eruptions, carbon dioxide and water vapour are ejected into the stratosphere with, very often, compounds of sulphur such as $H_2S$ and $SO_2$ in gaseous form. The quantity of carbon dioxide ejected in a typical eruption is thought to be only about 0.01 ppmv, so the addition of carbon dioxide to the atmosphere is minute compared with the current rate of annual increase (1.5 ppmv). Likewise the heat output is, in relative terms, minute. It has long been considered, however, that the dust vented from a huge volcanic eruption that reaches well into the stratosphere could affect climate. This was thought to be likely because:

(a) Estimates of surface temperature over widespread parts of the globe often showed a drop after (but also, disturbingly often, before) a huge volcanic eruption.

(b) The measured intensity of the direct solar beam was always reduced though the diffuse radiation usually increased to partially compensate.

The classic book on volcanic dust and climate is by Humphreys (1940), whose ideas are instructive and not wholly outdated. An extensive description of the development of observational studies of climatic effects in relation to volcanic dust is given by Lamb (1972). Fig 3.12, from Lamb (1972) shows examples of historical measurements of monthly average values of the strength of the direct solar beam, while Fig 3.13 shows graphs of historic regional average temperatures derived by Koppen (see p 410ff of Lamb (1972)). The timing of the largest volcanic eruptions is shown on the diagrams. Lamb has devised a "dust veil" index to measure the climatologically most important eruptions. The index is partly based on

observations of the optical effects of the dust but also on the worldwide fall in surface temperature (as far as it can be judged) following a given eruption (Lamb (1970)). This subjective index suggests that the eruptions of Tambora (1815) (Indonesia), Coseguina (1835) (Nicaragua), Krakatau (Indonesia) (1883) and Agung (Indonesia) (1963) (Fig 3.14) were among those most likely to have affected surface temperatures since the beginning of the nineteenth century, prior, that is, to the recent eruption of El Chichon (see below). On a millenial time scale, Fig 3.15, from Lamb (1972), shows an apparent association between the reconstructed extent of sea-ice near Iceland and volcanic eruptions in Iceland. Acidity measurements in cores from polar ice sheets have now been used to infer volcanic records for past centuries, and Legrand and Delmas (1987) have tentatively postulated that a hitherto unknown major eruption occurred around 1808, ie 7 years before Tambora (Fig 3.16). Hammer et al (1980) have obtained an acidity series stretching back to before 600 AD from the Greenland ice sheet.

### 3.3.2 Controversy concerning volcanic dust and climate

The problem of whether the apparent associations between volcanic activity and climate are real continues to be controversial. The main reasons for controversy are:-

(a) There may be sufficient variability between eruptions in the physics of the interaction between volcanic dust and solar and terrestrial long wave radiation that the sign of the effect of stratospheric volcanic dust on surface temperature may vary from eruption to eruption. The net effects depend crucially on the size distribution and chemical constitution of the dust, which may vary between eruptions.

(b) It has not yet proved possible to use an AGCM with a realistic stratosphere and including what would now be regarded as the essential physics of the radiative interactions, to attempt to simulate the

climatic effects of volcanic dust (Hofmann (1987)). In any case, the simulated response of the oceans could be crucial as volcanic 'dust' may stay in the stratosphere for several years.

It is now thought that the reason why past ground measurements have indicated long residence times for stratospheric dust, despite the appreciable scavenging that must exist through dynamical interactions between troposphere and stratosphere, is that some of the "dust" is formed after the eruption. Sulphur gases ($H_2S$, $SO_2$ etc) formed during the eruption may slowly combine with stratospheric water vapour to produce reflective, aqueous droplets of a typical diameter 1 μm or less whose terminal velocities are very low. So the quantity of sulphur gas and possibly sulphur particles ejected in an eruption is now thought to be very important. Lamb (1972) shows terminal velocities for spherical particles of several radii (Table 3.1).

Table 3.1 (from Lamb (1972))

STRATOSPHERIC RESIDENCE TIMES FOR VOLCANIC DUST

(Total times taken to fall through still air to tropopause at (a) 17 km, (b) 12 km)

| Particle Diameter | Initial height (km) | (a) | (b) |
|---|---|---|---|
| 2 μm | 40 | 25 weeks | 41 weeks |
| | 30 | 21 weeks | 37 weeks |
| | 25 | 16 weeks | 31 weeks |
| | 20 | 7 weeks | 23 weeks |
| 1 μm | 40 | 1.9 years | 3.1 years |
| | 30 | 1.6 years | 2.8 years |
| | 25 | 1.3 years | 2.4 years |
| | 20 | 0.6 years | 1.7 years |
| 0.5 μm | 40 | 7.8 years | 12.5 years |
| | 30 | 6.5 years | 11.3 years |
| | 25 | 5.0 years | 9.7 years |
| | 20 | 2.2 years | 6.9 years |

### 3.3.3 El Chichon

In April 1982 a very violent, explosive eruption occurred in S Mexico from the volcano El Chichon (the "lump on the head") situated at 17°N 93°W. Fig 3.17 from Robock and Matson (1983) shows how the dust from that explosion circled the globe in about 1 month in a narrow band between 15°-25°N. Winds were easterly, and accelerating, at the 25-30 km level where much of the dust initially resided because the summer stratospheric circulation was just getting underway. At Hawaii (Central Pacific 19°N) directly under the dust cloud, direct solar radiation was reduced by up to 30% in the months following the eruption, a reduction offset, but not completely, by an increase in diffuse solar radiation (De Luisi et al (1983)). The measurements indicated that in the visible spectrum the dust produced a mean optical depth T of the order of 0.25. Optical depth is defined by

$$F = F_o \, e^{-T} \qquad (3.8)$$

$F_o$ is the incident flux and F is that part of the flux that emerges below the dust layer without absorption or being scattered, i.e. F only measures the reduction of direct radiation. Balloon and other measurements suggested that a few months after the eruption much of the cloud was composed of droplets containing 75% sulphuric acid and 25% water with a mode radius of about 0.3 μm (MacCracken and Luther (1984) give details). There was also hydrochloric acid in the cloud (Hofmann (1987)). By July the dust cloud, now at a height of between 20-25 km, reached Italy. It became visible to the naked eye on a few evenings in August 1982 around Bracknell, with some unusual sunsets. Referring back to Table 3.1, droplets near a radius of 0.3 μm have terminal velocities so low that dynamical and other processes are likely to be important for their removal from the stratosphere, and the decay of the El Chichon stratospheric aerosol by a factor of 10 took about 2 years (Hofmann (1987)). Global surface temperatures rose soon after the eruption, because of El Nino (see Lecture 6). Parker (1985) compensated tropical tropospheric temperatures for the Southern Oscillation and found no clear evidence for

eruption-related cooling, but Angell (1988), using worldwide data, did find tropospheric and surface cooling after El Chichon and earlier eruptions when the influence of El Nino had been compensated for. Note, however, that volcanic eruptions may influence El Nino, and also the Indian Monsoon (Handler (1986)).

### 3.3.4 Heating of stratospheric dust layer

It is not completely obvious that a stratospheric volcanic dust cloud should become hotter than its environment. The particles may be so small that solar heating is negligible and their radiative properties could be such that infra-red radiation from below also has little effect. Newell (1981) claimed to have detected a heating of the dust cloud produced by Agung (1963) by several degrees centigrade. Theoretical work (e.g Pollack et al (1976); Vupputuri and Blanchet (1984)) has suggested that a heating of several degrees is possible for the likely sizes and chemical constituents of volcanic dust, mainly due to the absorption of infra-red radiation from below. Parker and Brownscombe (1983) cautiously concluded that the El Chichon dust cloud was heated near the equator between 30-50 mb by several degrees centigrade. Fig 3.18A (from Parker and Brownscombe (1983)) shows stratospheric temperatures at several levels in 1980-82 derived from the NOAA 6 Stratospheric Sounding Unit and Microwave Sounding Unit. Of the levels sampled, that at 50 mb shows the largest temperature increase from 1981-82. Fig 3.18B, (again from Parker and Brownscombe) shows the 30 mb temperature anomalies in August 1982 from radiosonde data. A complicating factor in this and the Agung studies is that anomalous warming was expected in both 1963 and 1982 within 15°N or S of the equator below the descending, westerly, phase of the stratospheric "quasi-biennial oscillation" (QBO) (see Lecture 6). However, an analysis by Labitzke et al (1983) of the 50 and 30 mb temperatures between 1964 and 1982 strongly suggests that the QBO contributed only a part of the 1982 warming. The location of the observed temperature anomaly maximum near the equator in Fig 3.18B, rather than at the latitude of the main dust cloud (20°N), is probably partly a result of the additional influence of the QBO.

### 3.3.5 A schematic, simplified, model of effects of volcanoes on surface temperature

Although literature on the modelling of the physical effects of volcanic dust on the surface temperature is in some disagreement, there is an emerging picture of the important physical processes. However the sign of the effect of volcanic dust in the surface energy balance is difficult to determine because there are two important competing physical effects and a host of smaller ones. The most important opposing effects are:-

(a) The dust layer reflects solar radiation, tending to cool the surface of the earth.

(b) The dust layer absorbs terrestrial radiation, tending to warm the surface of the earth.

Absorption of solar radiation can be significant but is now thought to be fairly small, at least in some volcanic eruptions.

Fig 3.19 shows a simple schematic model which cannot be used to make predictions. Because we shall estimate the perturbation of the surface energy balance resulting from stratospheric dust, we will not explicitly include the effects of carbon dioxide and other greenhouse gases which are assumed to be fixed. Imagine solar radiation I passing down through the dust layer; a fraction rI is reflected to space and lost while the remaining fraction tI = (1-r)I is transmitted to ground either as direct or diffuse radiation. Here we have assumed no absorption of solar radiation by the dust layer itself, which is not quite correct. The transmitted radiation, It, reaches the "ground" and a fraction $\alpha$It, is reflected upward: strictly speaking, the albedo $\alpha$ is not quite the same as for the "non dust" case as more of the solar radiation is diffuse and less is direct. On reaching the dust layer again, an amount of reflected radiation t($\alpha$It) is lost and an amount r($\alpha$It) is reflected down. So the initially reflected solar radiation is multiply -reflected between dust layer and ground with rapidly decreasing intensity. The initial loss of solar

radiation to the system, rI, is to some extent "made up" by the multiple reflections as the expected radiation loss from the ground in the absence of dust (for a non-zero value of $\alpha$) is clearly reduced. However the total radiation absorbed by the ground cannot quite reach the initial amount transmitted (It) for a non-zero value of $\alpha$.

Now also assume that a fraction b of the long-wave radiation U lost from the surface (partly indirectly from the troposphere itself - see Section 3.2) is absorbed by the dust layer without further reflection.

Then we find that the solar radiation absorbed by the ground $I_G$ is:-

$$I_G = (1-\alpha)tI \quad (1+r\alpha+r^2\alpha^2+\ldots)$$

or $$I_G = \frac{(1-\alpha)tI}{1-r\alpha} \quad \text{after summation}$$

Similarly the solar radiation lost through the dust layer to space after multiple reflection is:-

$$I' = rI+t^2\alpha I \quad [1+r\alpha+\ldots]$$

or $$I' = I\left(r+\frac{t^2\alpha}{1-r\alpha}\right)$$

We can now calculate the value of $I_G$ . The radiation balance at the ground is:-

$$-B+U = I_G \qquad (3.9)$$

where B is the longwave radiation emitted by the dust layer and U is the longwave radiation emitted by the ground.

The radiation balance above the dust layer is

$$B+(1-b)U = I-I' \qquad (3.10)$$

Adding (3.9) and (3.10) and substituting for $I_G$ and I' we find

$$U = \left[\frac{2}{2-b}\right] I \left[\frac{1-r-\alpha+\alpha r}{1-r\alpha}\right] \qquad (3.11)$$

Now if t = 1 and r = 0, ie no dust layer exists, we found in Section 3.1.1 that U = (1-α)I (equation (1)). So the net change ΔU in the long-wave radiation lost (eventually) by the ground when a dust layer is interposed is:-

$$\Delta U = I(1-\alpha)\left\{\left[\frac{b}{1-r\alpha} + {}/_2\right](1-r)-1\right\} \qquad (3.12)$$

where b has been assumed to be small so that $\frac{1}{1-b/2} \simeq 1+{}^b/_2$

Now $U = \sigma T_g^4$ (approximately) as in section 3.2.1, so $\Delta U = 4\sigma T_g^3 \Delta T_g$. Table 3.2 shows calculations of equilibrium values of $\Delta T_g$, assuming $T_g$ = 287°C, for reasonable values of t and b. The effects of additional surface evaporation etc are neglected. MacCracken and Luther (1984), Pollack et al (1976) and Chou et al (1984) give a discussion of the detailed physics and its uncertainties and suggestions for values of t, (dust layer transmission coefficient), and b (dust layer absorption coefficient) and their effects on surface temperature.

TABLE 3.2 EQUILIBRIUM TEMPERATURE CHANGES AT THE SURFACE FROM THE SCHEMATIC MODEL, °C

1. b = 0

| α | t = 0.99 | t = 0.97 | t = 0.95 |
|---|---|---|---|
| 0 | -0.6 | -1.9 | -3.1 |
| 0.3 | -0.3 | -0.9 | -1.6 |
| 0.6 | -0.1 | -0.3 | -0.5 |
| 0.8 | 0.0 | -0.1 | -0.1 |

2. b = 0.02

| α | t=0.99 | t=0.97 | t=0.95 |
|---|---|---|---|
| 0 | 0.0 | -1.3 | -2.6 |
| 0.3 | 0.1 | -0.5 | -1.1 |
| 0.6 | 0.2 | -0.3 | -0.3 |
| 0.8 | 0.1 | +0.1 | 0.0 |

It is seen that the sign of the change in surface temperature is very sensitive to t and to b and also to $\alpha$. These results agree qualitatively with existing ideas, despite the crudeness of the model. A cooling due to volcanic dust is less likely where $\alpha$ is high; and small changes in b, the coefficient that measures the absorption by the dust of long-wave radiation, can easily change the sign of a surface temperature response. Chou et al (1984) agree that eruptions are likely to produce varying surface temperature responses as a result of differences in particle size or chemical composition even if their dust clouds are similar in extent and optical depth. The temperature changes in Table 3.2 would be much reduced in practice because of the thermal inertia of the oceans. Fig 3.20 from Chou et al (1984) is a simple (but very uncertain) time-dependent calculation making some allowance for oceanic thermal inertia and the decay with time of the dust layer. In Lectures 8 and 9 we consider briefly whether it is likely that volcanic dust has really affected surface and tropospheric temperature in recent centuries.

REFERENCES TO LECTURE 3

ANGELL, J K (1988) Impact of El Nino on the delineation of tropospheric cooling due to volcanic eruptions. J. Geophys. Res., 93, D4, 3697-3704.

BERGER, A (1984) Accuracy and frequency stability of the Earth's orbital elements during the Quaternary. Milankovitch and Climate, Pt. I: Ed. A Berger et al, NATO ASI 126, (D. Reidel Pub. Co.), pp 3-39.

BERGER, A and PESTIAUX, P (1984) Accuracy and stability of the Quaternary terrestrial insolation. Milankovitch and Climate Pt 1. Ed: A Berger et al, NATO ASI, 126, (D. Reidel Pub. Co.), pp 83-111.

BORISENKOV, YE. P, TSVETKOV, A V and AGAPONOV, S V (1983) On some characteristics of insolation changes in the past and the future. Climatic Change, 5, 237-244.

CALDER, N (1974) The Weather Machine. BBC, London.

CHOU, M-D, PENG, L, and ARKING, A (1984) Climate Studies with a multilayer energy balance Model, Pt III: Climatic impact of stratospheric volcanic aerosols. J. Atm. Sci., 41, 759-767.

DE LUISI, J J, DUTTON, E G, COULSON, K L, DEFOOR, T E and MENDONCA, B G (1983) On some radiative features of the El Chichon volcanic stratospheric dust cloud and a cloud of unknown origin observed at Mauna Loa. J. Geophys. Res., 88, C11, 6769-6772.

DONNELLY, R F (1983) Solar UV spectral irradiance variations. In 'Weather and Climate responses to solar variations'. Ed: B M McCormac, Colorado Ass. Univ. Press, pp 43-55.

EDDY, J A (1983) A Historical review of solar variability weather and climate. In 'Weather and Climate Responses to solar variations'. Ed: B.M. McCormac, Colorado Ass. Univ. Press, pp 1-15.

GILL, A E (1982) Atmosphere-ocean dynamics. Academic Press, 664 pp.

GILLILAND, R L (1983) Climate change as a test of the influence of external perturbations. In 'Weather and Climate responses to solar variations'. Ed: B M McCormac, Colorado Ass. Univ. Press, pp 273-281.

HAMMER, C U, CLAUSEN, H B and DANSGAARD, W (1980) Greenland ice sheet evidence of post-glacial volcanism and its climatic impact. Nature, 288, 230-235.

HANDLER, P (1986) Stratospheric aerosols and the Indian Monsoon. J. Geophys. Res, 91, D13, 14475-14490.

HENDERSON-SELLERS, A and McGUFFIE, K (1987) A climate modelling primer. Chichester (Witley), 217pp

HOFMANN, D J (1987) Perturbations to the global atmosphere associated with the El Chichon volcanic eruption of 1982. Rev. Geophys., 25, 743-759

HUDSON, H S (1983) Variations of the Solar Radiation Input. In 'Weather and Climate responses to solar variations'. Ed: B M McCormac, Colorado Ass. Univ. Press, pp 31-41.

HUMPHREYS, W J (1940) Physics of the air. 3rd Edition. Reprinted by Dover (1964).

KOPPEN, W (1873) Ueber Mehrjahrige Perioden der Witterung, insbesondere uber die 11-jahrige Periode der Temperatur. Z. Met., Vienna, 8, pp 241-248, 257-267.

KOPPEN, W (1914) Lufttemperaturen, Sonnenflecke und vulkanausbruche. Met., Z. Braunschweig, 31, pp 305-328.

LABITZKE, K, NAUJOKAT, B, and McCORMICK, M P (1983) Temperature effects on the stratosphere of the April 4, 1982, eruption of El Chichon, Mexico. Geophys. Res. Letters, 10, 24-26.

LAMB, H H (1970) Volcanic dust in the atmosphere. Phil Trans, Roy Soc, A, 266 (No 1178) pp 426-533.

LAMB, H H (1972) Climate, Present, Past and Future. Vol 1, Methuen.

LAPLACE, P S (1798) Traité de Mécanique Céleste. 5 Vols. Paris (4th Ed., Paris, 1882).

LEGRAND, M and DELMAS, R J (1987) A 220-year continuous record of volcanic $H_2SO_4$ in the Antarctic ice sheet. Nature, 327, 671-676.

MacCRACKEN, M C and LUTHER, F M (1984) Radiative and climate effects of the El Chichon eruption. Proc of Fifth Amer. Met. Soc. Conf. Radiation, 31 October-4 November 1983, Baltimore MD.

MASON, B J (1976) Towards the understanding and prediction of climatic variations. Quart.J. Roy. Met. Soc., 102, 473-498.

MILANKOVITCH, M (1941) Canon of insolation and the ice age problem - Spec. Pub. 132, Trans. No. 1793, 1969 - Israel Program for Scientific Translations.

MORRISON, L V, STEPHENSON, F R and PARKINSON, J (1988) Diameter of the sun in AD 1715. Nature, 331, 421-423

NATIONAL ACADEMY OF SCIENCES (1975) Understanding Climatic Change. Washington DC

NATIONAL RESEARCH COUNCIL (1982) Solar Variability, Weather and Climate. Ed: J Eddy. Studies in Geophysics Ser., Geophys. Res. Board. National Academy Press.

NEWELL, R E (1981) Further studies of the atmospheric temperature change produced by the Mt Agung volcanic eruption in 1963. J. Volcanology and Geothermal Research, 11, 61-66.

NEWHALL, C G and SELF, S (1982) The volcanic explosivity index (VEI): An estimate of explosive magnitude for historical volcanism. J. Geophys. Res., 87, 1231-1238.

PARKER, D E (1985) The influence of the Southern Oscillation and volcanic eruptions on temperature in the tropical troposphere. J. Climatology, 5, 273-282.

PARKER, D E and BROWNSCOMBE, J L (1983) Stratospheric warming following the El Chichon volcanic eruption. Nature, 301, 406-408.

POLLACK, J B, TOON, O B, SAGAN, C, SUMMERS, A, BALDWIN, B, and VAN CAMP, W (1976) Volcanic Explosions and Climatic Change: A theoretical assessment. J. Geophys. Res, 81, 1071-1083.

RAMPINO, M R and SELF, S (1982) Historic eruptions of Tambora (1815), Krakatau (1883), and Agung (1963), their stratospheric aerosols, and climatic impact. Quaternary Research, 18, 127-143.

RASCHKE, E, VONDER HAAR, T H, BANDEEN, W R and PASTERNAK, M (1973) The annual radiation balance of the earth-atmosphere system during 1969-70 from Nimbus 3 measurements. J. Atm. Sci., 30, 341-364.

RIBES, E, RIBES, J C and BARTHALOT, R (1987) Evidence for a larger sun with a slower rotation during the seventeenth century. Nature, 326, 52-55.

ROBOCK, A and MATSON, M (1983) Circumglobal transport of the El Chichon volcanic dust cloud. Science, 221, 195-197.

STEPHENS, G L, CAMPBELL, G G and VONDER HAAR, T H (1981) Earth radiation budgets. J. Geophys. Res., 86, C10, 9739-9760.

VUPPUTURI, R K R and BLANCHET, J P (1984) The possible effects of El Chichon eruption on atmospheric thermal and chemical structure and surface climate. Geofis. Int., 23-3, 433-447.

WILLSON, R C (1982) Solar irradiance variations and solar activity. J. Geophys. Res., 87, A6, 4319-4326.

WILLSON, R C and HUDSON, H S (1988) Solar luminosity variations in solar cycle 21. Nature, 332, 810-812.

WINSTON, J S, GRUBER, A, GRAY, T I, VARNADORE, M S, EARNEST, C L and MANNELLO, L P (1979) Earth-atmsophere radiation budget analyses derived from NOAA satellite data June 1974 - February 1978. Vols 1 and 2, US Dept of Commerce, Washington DC.

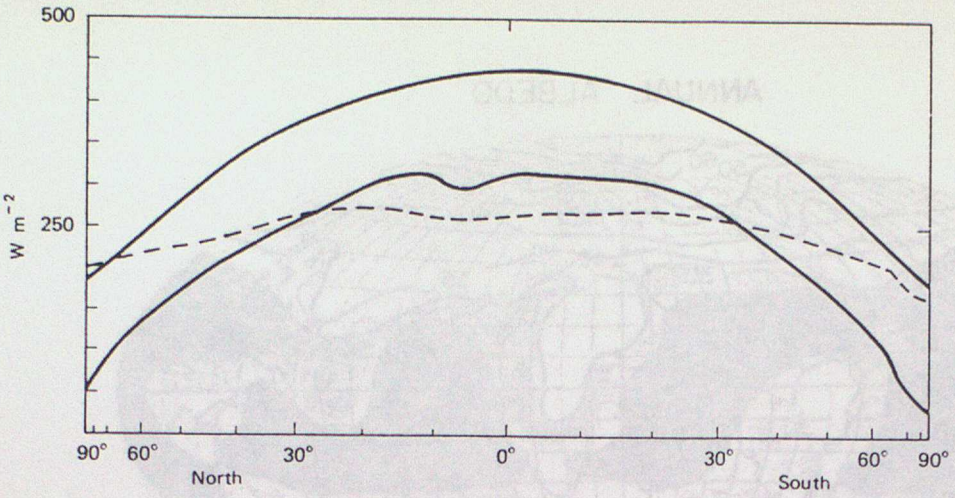


The radiation balance of the earth. The upper solid curve shows the average flux of solar energy reaching the outer atmosphere. The lower solid curve shows the average amount of solar energy absorbed; the dashed line shows the average amount of outgoing radiation. The lower curves are average values from satellite measurements between June 1974 and February 1978, and are taken from Volume 2 of Winston *et al.* (1979). Values are in watts per square meter. The horizontal scale is such that the spacing between latitudes is proportional to the area of the earth's surface between them, i.e., is linear in the sine of the latitude.

Figure 3.1A. From Gill (1982).

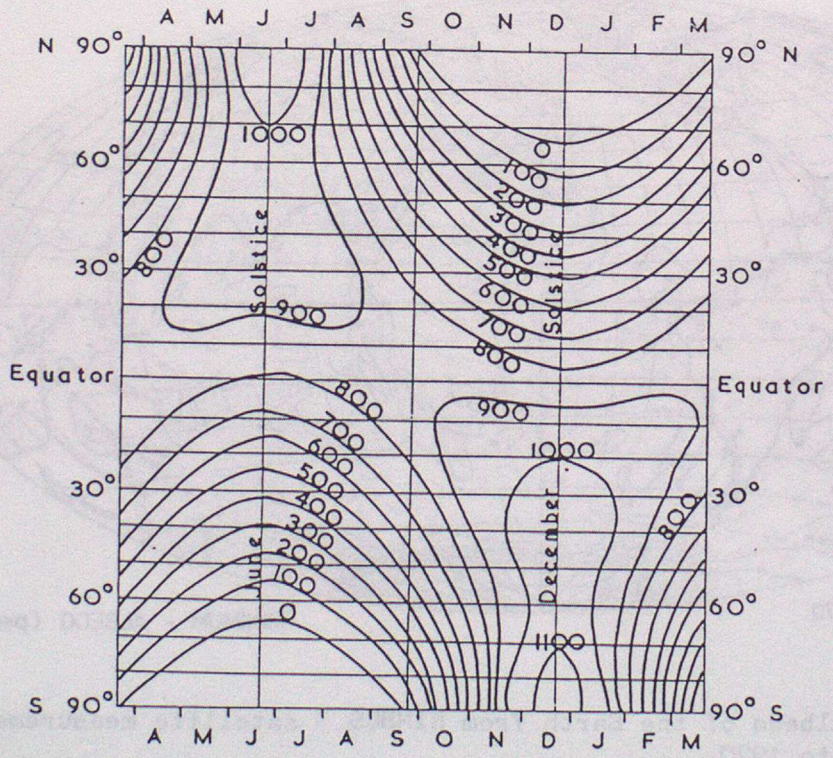


Daily totals of solar radiation available in different latitudes of the Earth in the absence of the atmosphere, in g cal/cm², around the year, at the present epoch. Divide by 2.07 to give $Wm^{-2}$.

Figure 3.1B. From Lamb (1972).

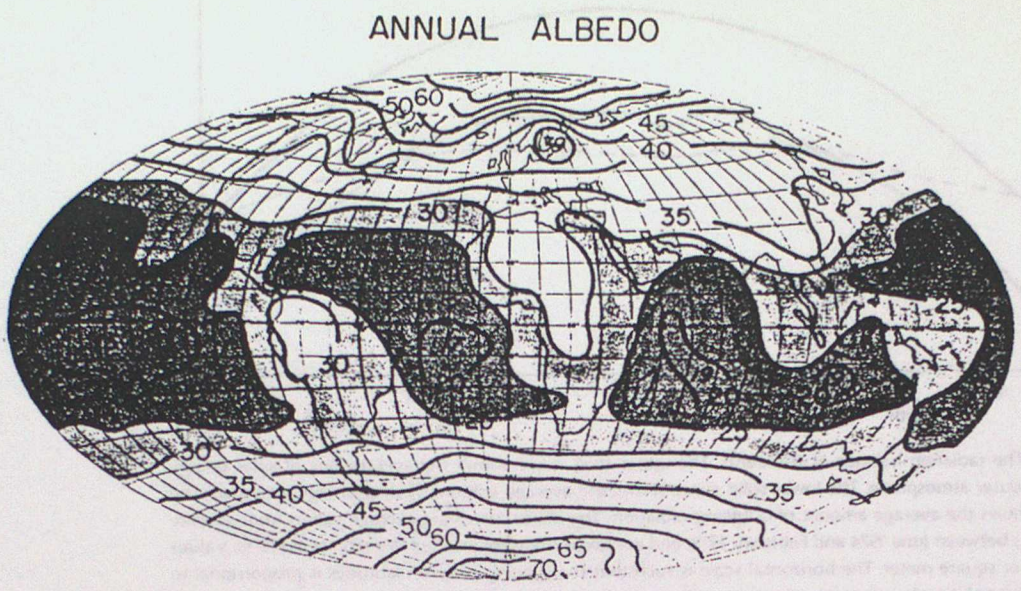


Figure 3.2. The average albedo obtained from a composite of 48 months of satellite data obtained between 1964 and 1977.
From Stephens et al (1981).

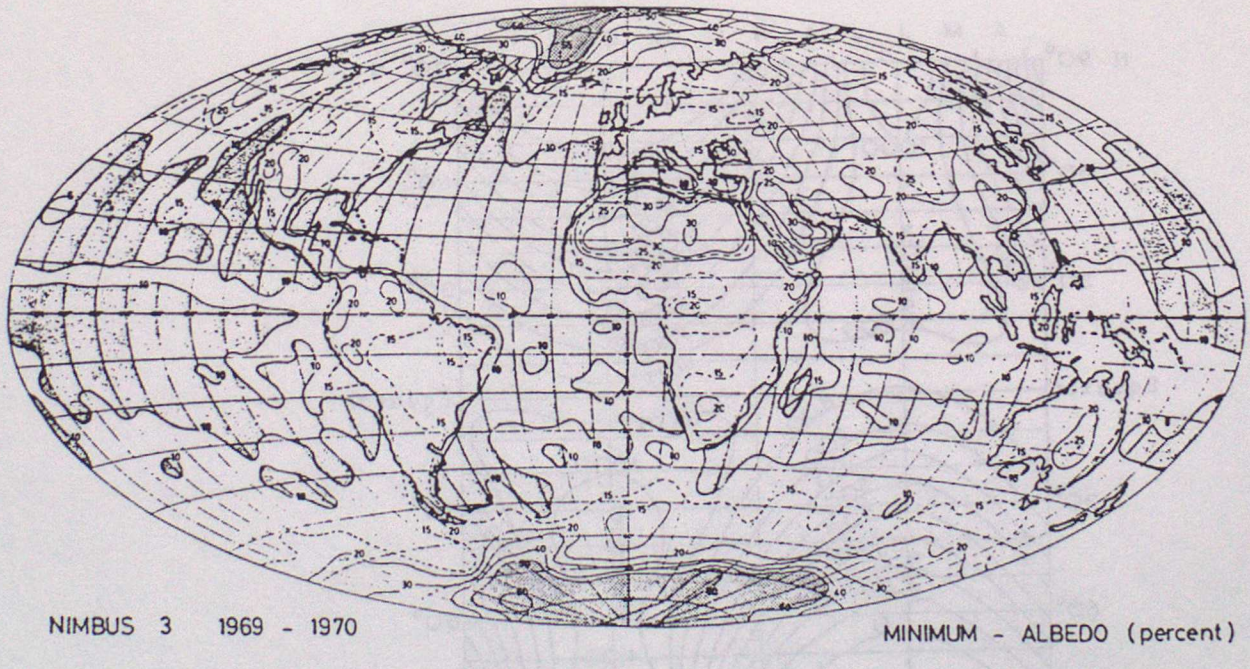


Figure 3.3. The minimum albedo of the Earth from NIMBUS 3 satellite measurements made in 1969 to 1970.
From Raschke et al (1973).

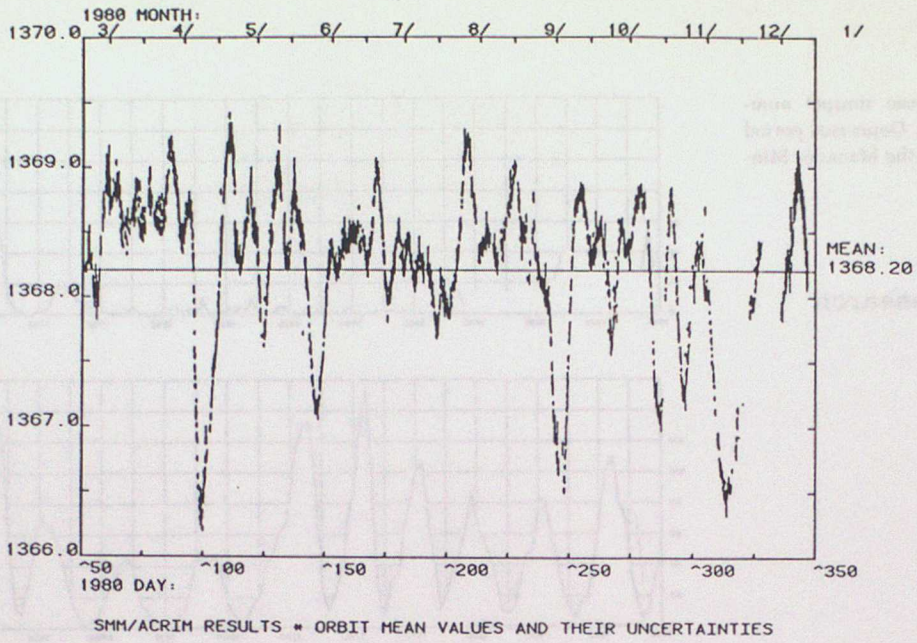


*Total solar irradiance (W m$^{-2}$) as measured by the active cavity radiometer onboard the SMM (Willson, 1982). Each point represents the average of data for one orbit (~96 min); the observed standard deviation for each point is on the order of 15 ppm. The large dips are associated with the crossing of the solar disk by large sunspot groups.*

Figure 3.4. From Hudson (1983).

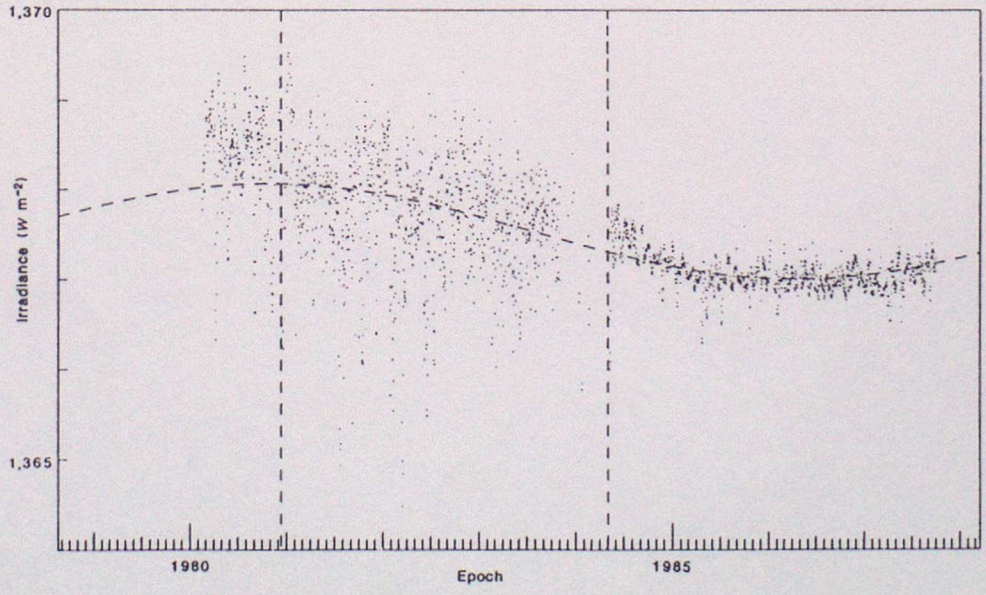


ACRIM I daily mean data from early 1980 to late 1987. The dashed vertical lines separate the two 'precision solar pointed' periods (most of 1980 and after March 1984) from the intervening 'spin-mode' period. The dashed curve is a fitted least-mean-square cosine function,

$$S = S_0(1 + 0.039 \times \cos(2\pi(t\text{-}1980.82)/10.95));$$

period 4,000 d; offset 300 d; amplitude $0.039 \pm 0.003\%$.

Figure 3.5. From Willson and Hudson (1988).

Annual mean sunspot numbers A.D. 1610 to present. Depressed period from about 1645 to 1715 is the Maunder Minimum.

Figure 3.6.

From National Research Council (1982).

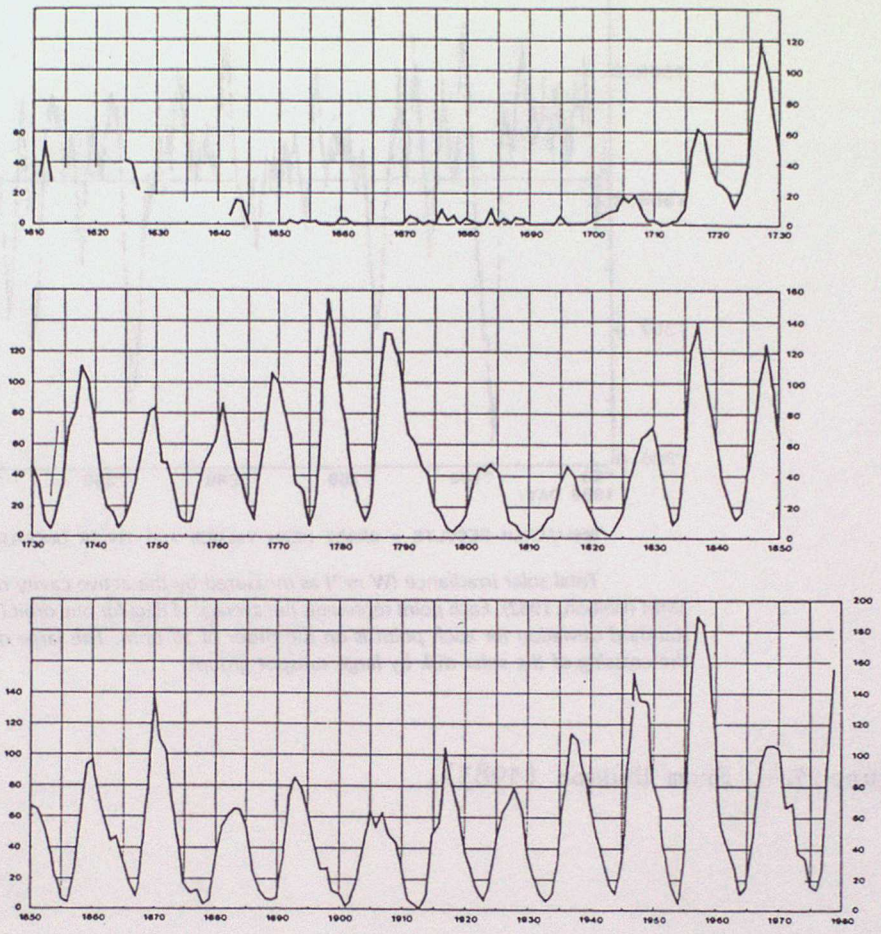

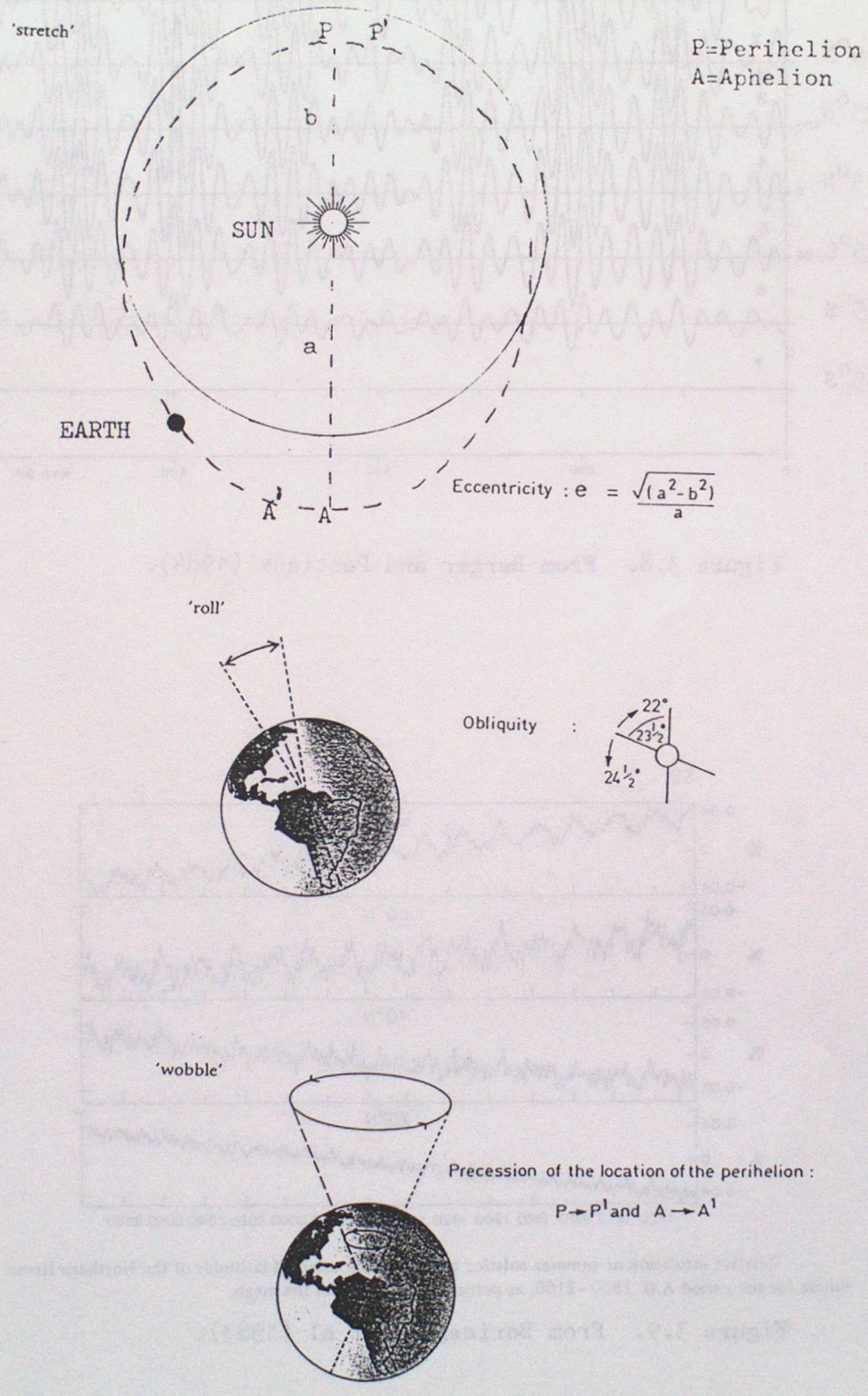


Figure 3.7. Variations in the earth's orbit.
Adapted from Calder (1974) and Henderson-Sellers and McGuffie (1987).

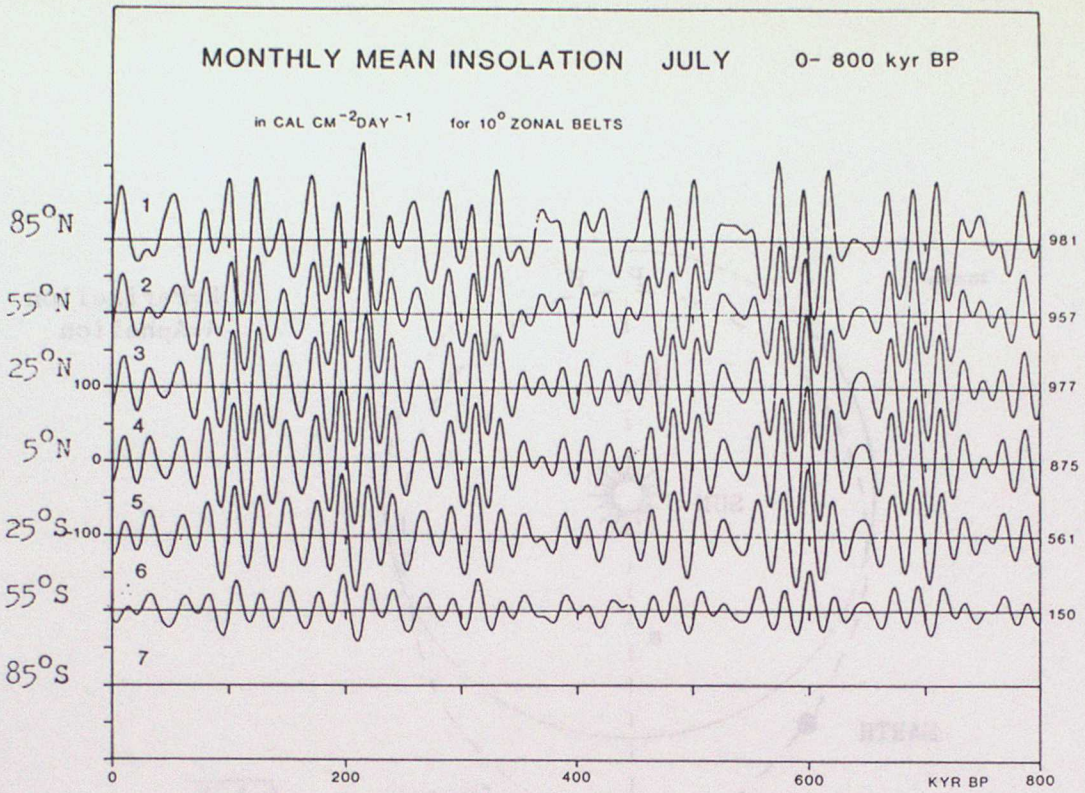


Figure 3.8. From Berger and Pestiaux (1984).

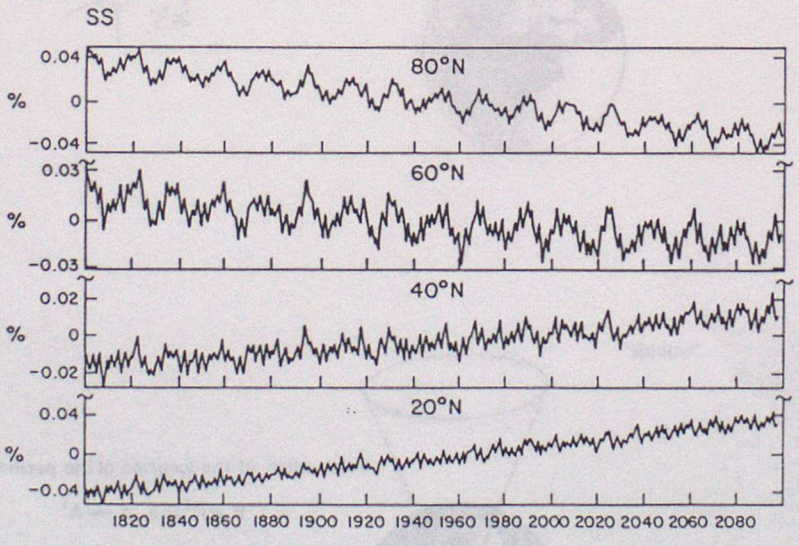


Relative insolation at summer solstice calculated for selected latitudes of the Northern Hemisphere for the period A.D. 1800–2100, as percent variation from the mean.

Figure 3.9. From Borisenkov et al (1983).

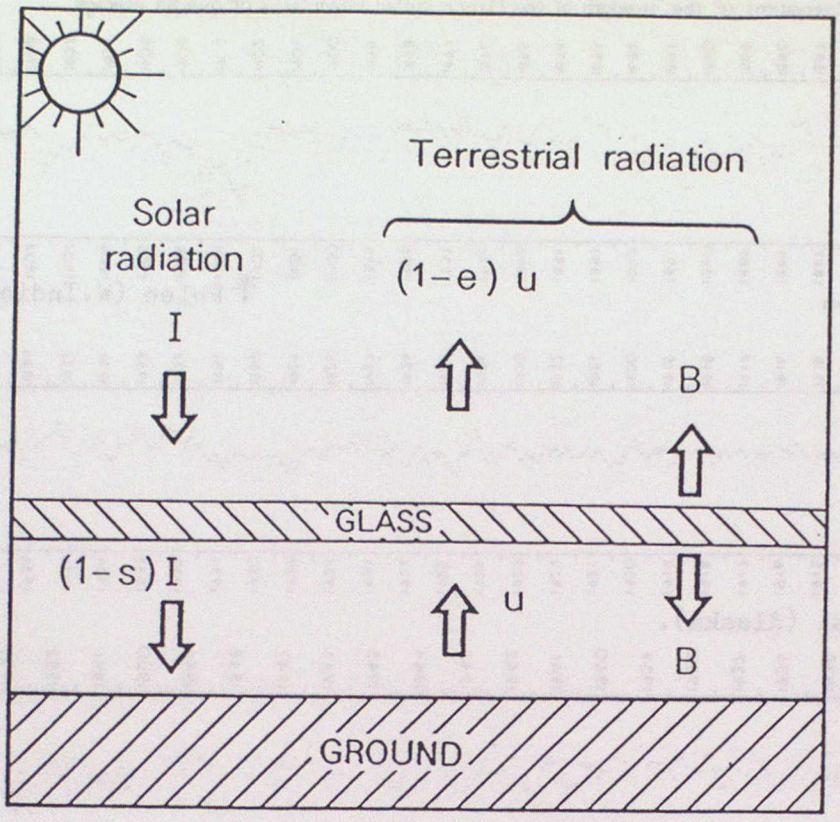


Fig. 3.10 The 'Greenhouse' effect

Adapted from Gill (1982)

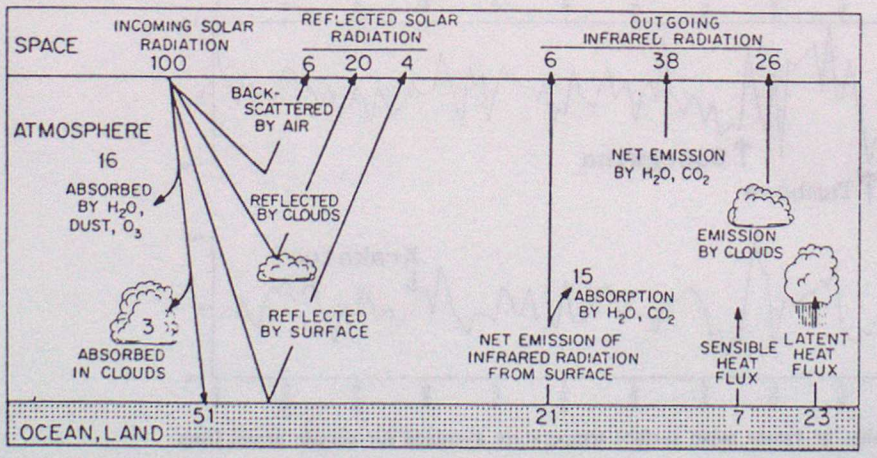


Radiation balance for the atmosphere. [Adapted from "Understanding Climatic Change," U.S. National Academy of Sciences, Washington, D.C., 1975, p. 14, and used with permission.]

Figure 3.11. From Gill (1982).

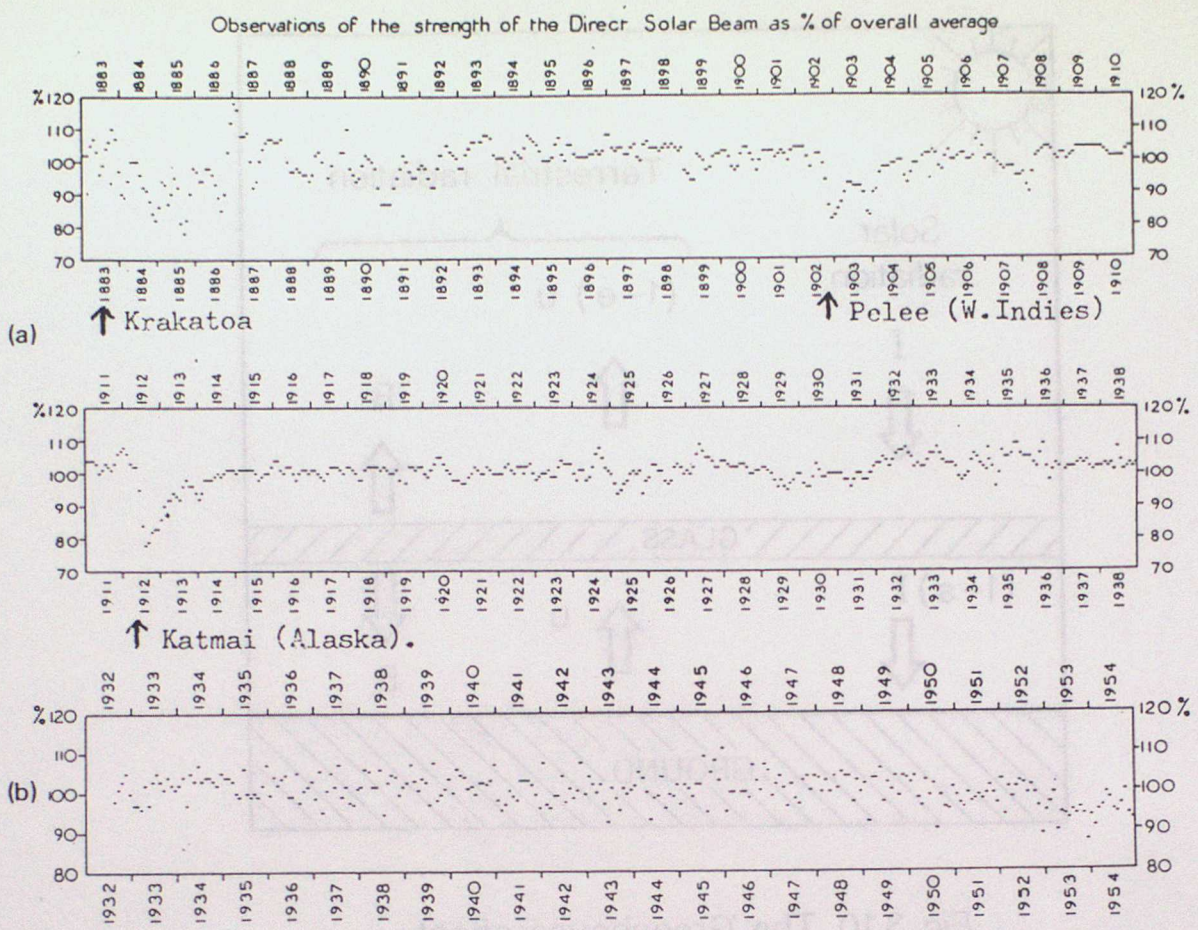


Fig. 10.16(*a*) Average monthly values of the strength of the direct solar radiation derived from observations at mountain observatories between 30° and 60°N in America, Europe, Africa and India from 1883 to 1938, as percentage of the overall mean.

(*b*) Average monthly values of the strength of the direct solar radiation derived from observations at Matsumoto (36°15′N, 137°58′E) and Shimizu (32°47′N, 132°58′E) in southern Japan from 1932 to 1954, as percentage of the overall mean.

Figure 3.12. From Lamb (1972).

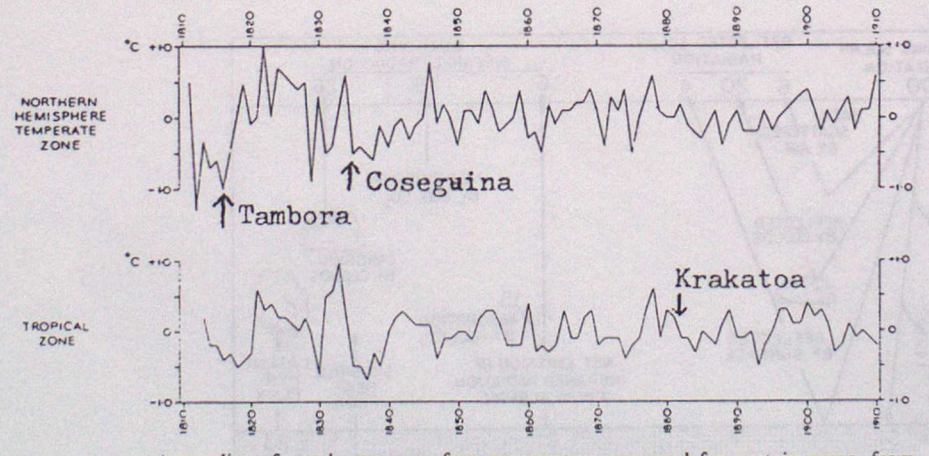


Anomalies of yearly mean surface temperature averaged for certain areas, from 1815 to 1910:

(*a*) Northern hemisphere temperate zone

(*b*) Tropical zone

Unsmoothed yearly values.

Standard deviations of the yearly values here plotted:

Northern temperate zone (land stations) 0·38°C.

Tropical zone (land stations) 0·29°C.

(*After* KÖPPEN *1873, 1914.*)

Figure 3.13. From Lamb (1972).

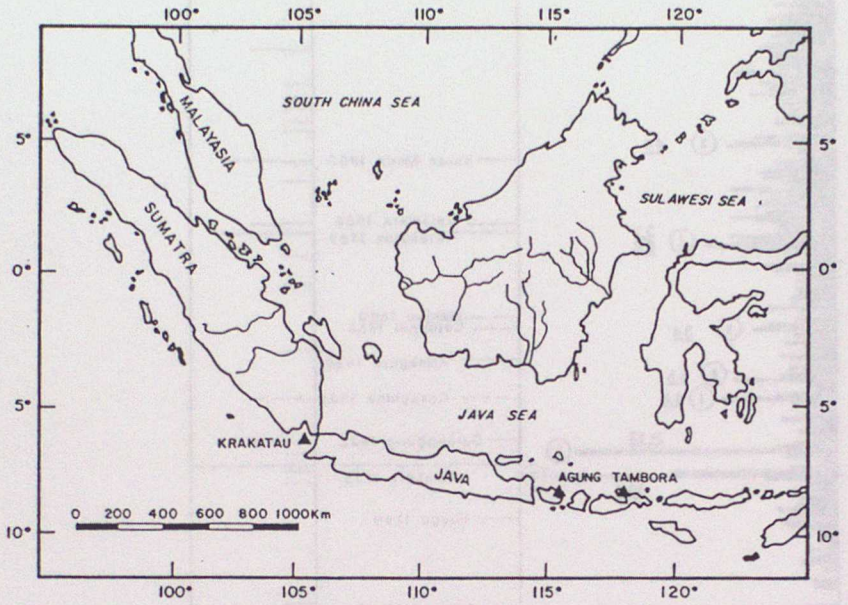


Map showing location of the three Indonesian eruptions discussed here: Tambora (1815), Krakatau (1883), and Agung (1963). (triangles).

Figure 3.14. From Rampino and Self (1982).

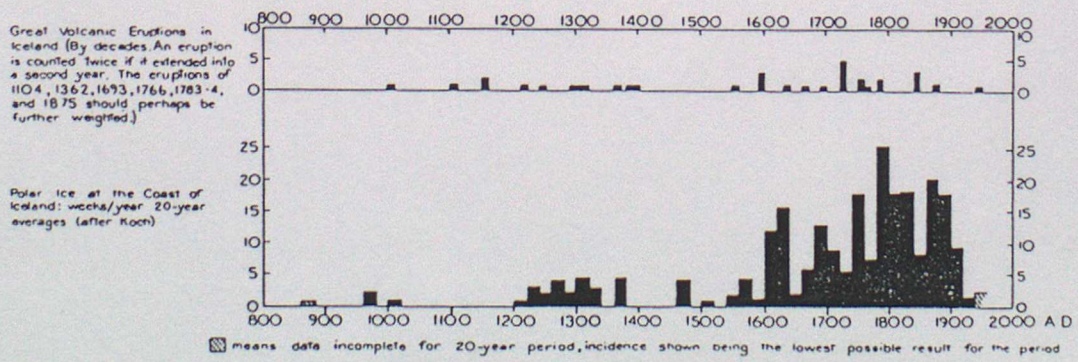


Great volcanic eruptions in Iceland and incidence of Arctic sea ice in that area since A.D. 870.

Figure 3.15 From Lamb (1972).

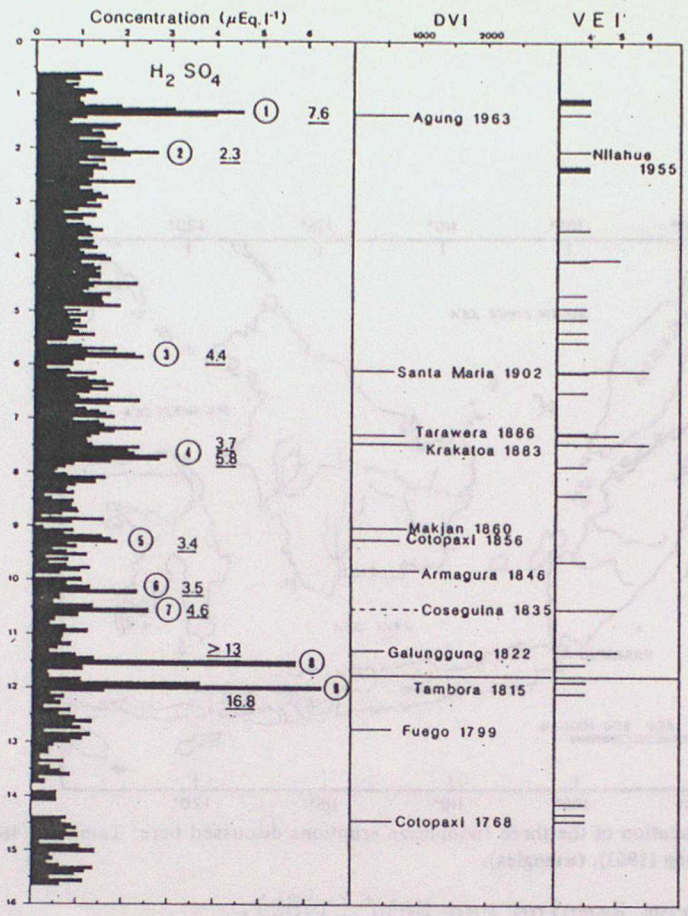


$H_2SO_4$ profile obtained at Dome C for the past 200 yr compared with the records of explosive volcanic eruptions south of 20° N. VEI (volcanic explosivity index) values are from ref. 6* and DVI (dust veil index) values are from ref. 5.* Major $H_2SO_4$ spikes, numbered 1 to 9, are of volcanic origin. The corresponding $H_2SO_4$ amount deposited at Dome C for each of these events is also indicated (underlined values, in kg $km^{-2}$).

* Ref 5 is Lamb (1970) and Ref 6 is Newhall and Self (1982).

Figure 3.16. From Legrand and Delmas (1987).

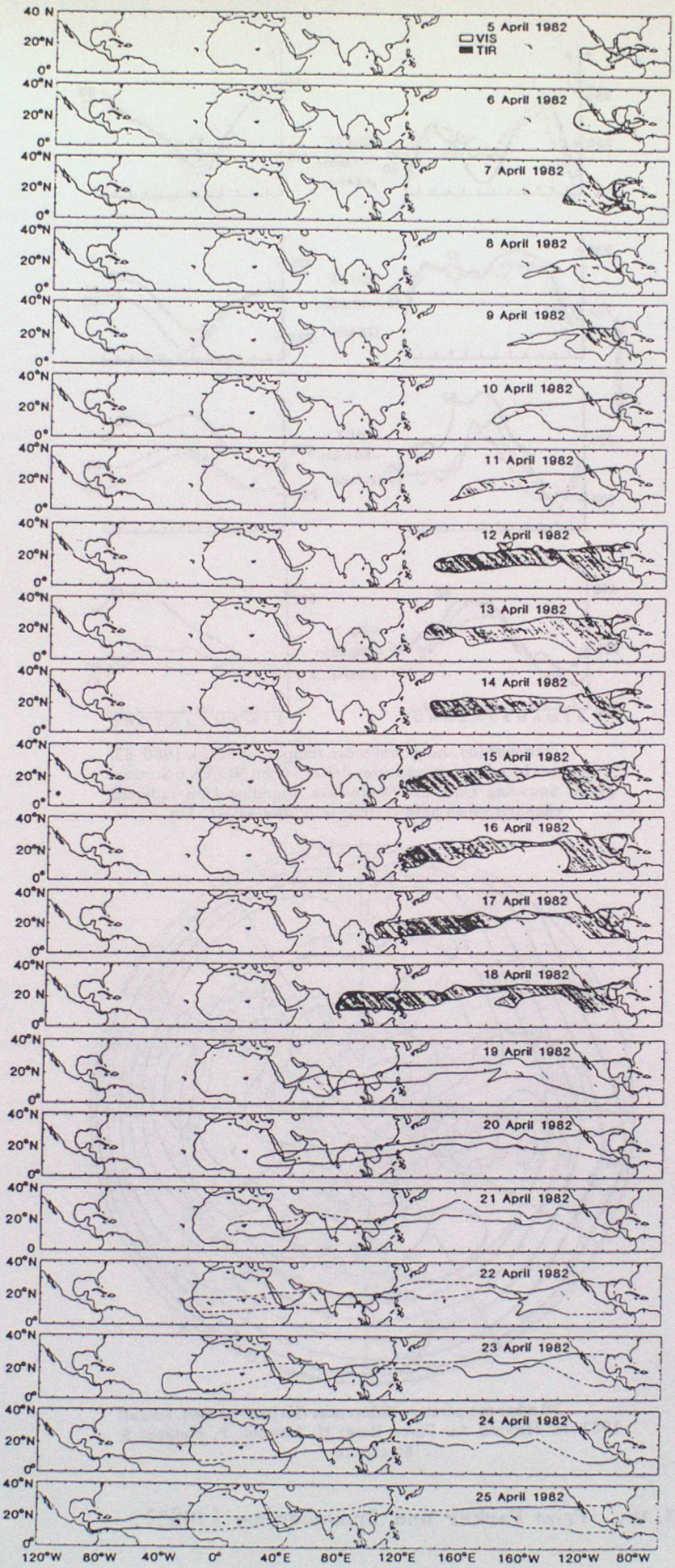


Figure 3.17. Location of the dust cloud from the El Chichon eruption as observed with visible (VIS) and thermal infrared (TIR) imagery. Portions of the cloud to the right of 180° are plotted at 0000 GMT. Portions to the left of 180° are plotted at 1500 local time. Dash-dot lines indicats difficulies in observing the exact location of the edge of the cloud. From Robock and Matson (1983).

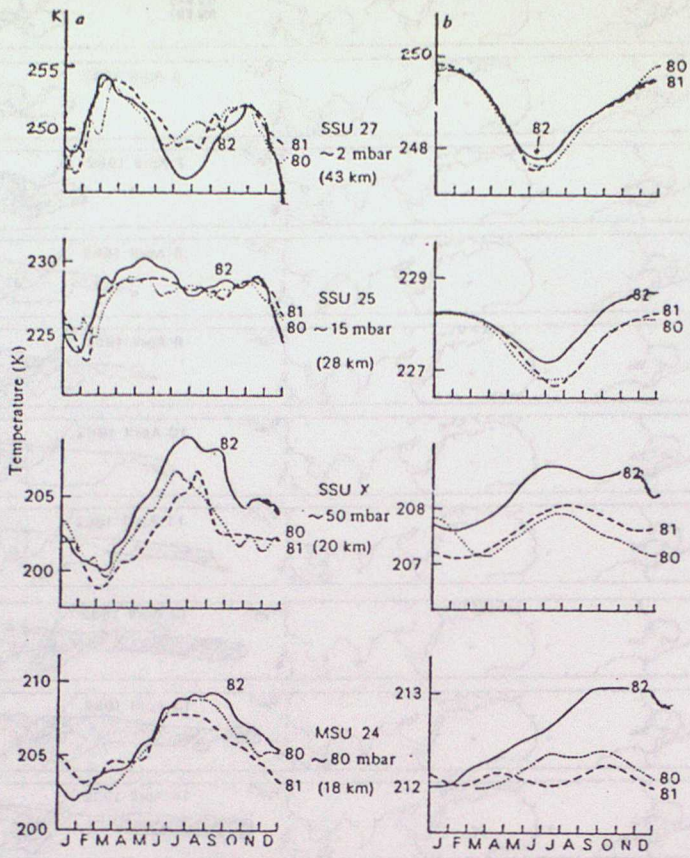


Tropical (*a*) and global mean temperatures (*b*), 1980–82. Values are based on temperatures derived from NOAA 6 Stratospheric Sounding Unit and Microwave Sounding Unit radiance channels which have vertical resolution of ~15 km.

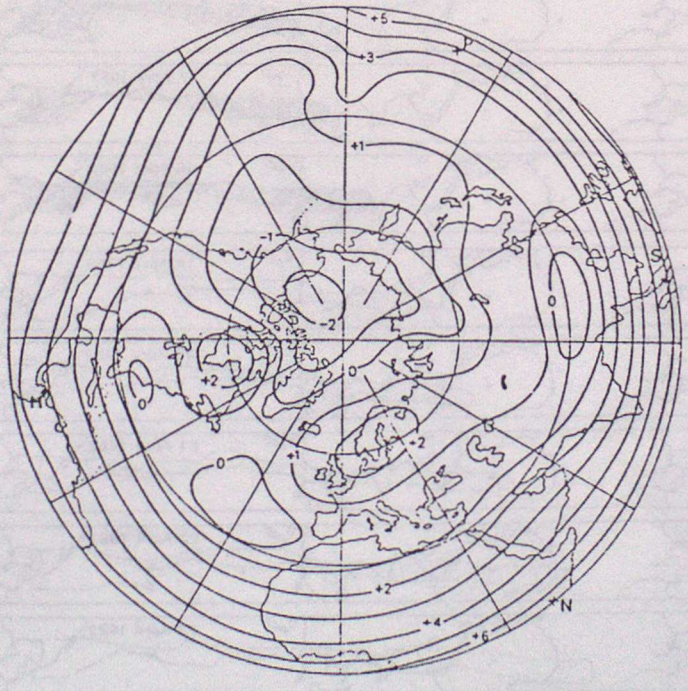


30 mbar temperature differences (K) from normal, August 1982. H, Howard Air Force Base; N, Nairobi; P, Ponape; S, Singapore.

Figure 3.18. From Parker and Brownscombe (1983).

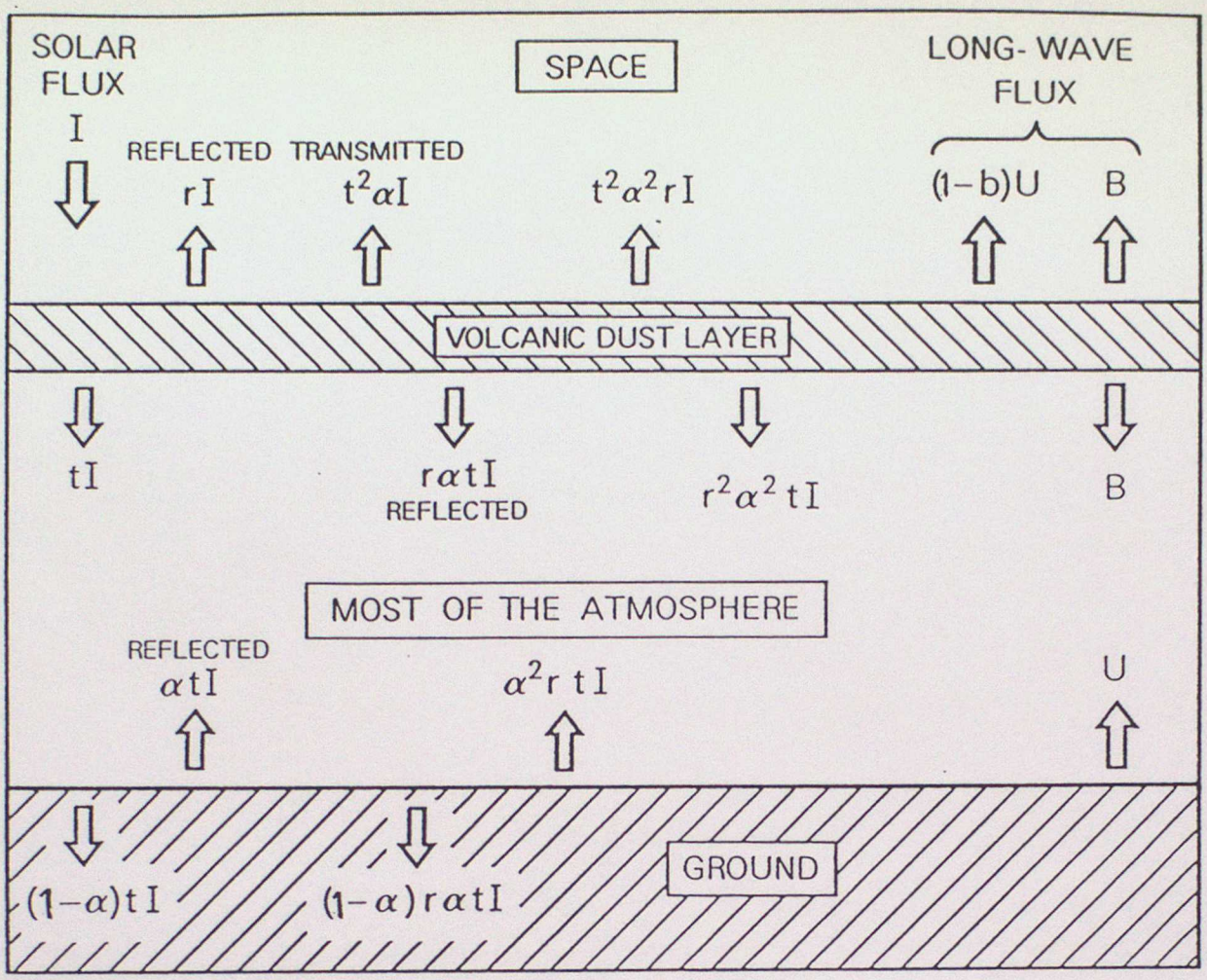


Fig. 3.19 Simple model of the effect of volcanic dust on surface radiation balance.

DO 3723

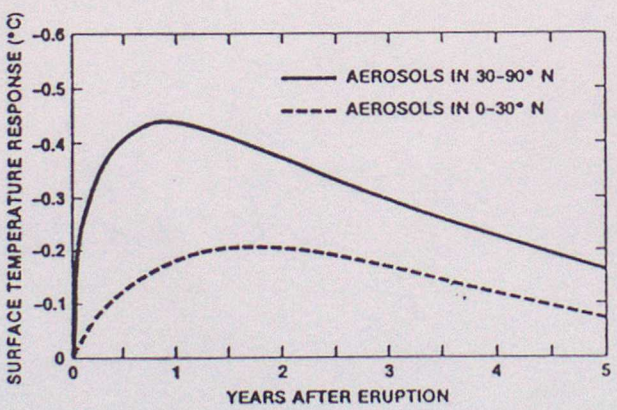


The response of the hemispherically averaged surface temperature to a uniform distribution of aerosols in the 30–90°N region (solid curve) and in the 0–30°N region (broken curve). The optical thickness of the aerosols is the same as in Fig. 7. of Chou et al(1984)

Figure 3.20 (From Chou et al (1984))

ADVANCED LECTURE NO 4

# CLIMATIC FORCING AND FEEDBACK PROCESSES

## II. INTERACTIONS WITH THE LAND SURFACE

C K FOLLAND and D E PARKER

MET O 13

SUMMARY

In this lecture we consider the role of persistent variations of soil moisture and land surface albedo in forcing or perpetuating anomalies of climate. The availability of soil moisture to the atmosphere depends on the vegetation cover as well as on climate, and is therefore sensitive to agricultural practices. Albedo is also a function of vegetation as well as of surface land type and snow-cover. A general introduction to the effects of variations of soil moisture and albedo on climate is followed by a selection of results from atmospheric general circulation model experiments.

### 4.1 INTRODUCTION

It has long been known that the albedo of the ground is affected by both the soil moisture and the vegetation cover. If the ground dries up sufficiently, it tends to increase in albedo; a further increase in albedo will result if the vegetation dies. Herein lies the potential for a feedback between the land surface and the climate, because the albedo determines the heat balance which can affect the atmospheric circulation: this in turn influences the rainfall, which has a major impact on the soil moisture and the vegetation cover.

Charney (1975) wrote an important paper which contained a simple dynamical model of drought-albedo feedback. Firstly, he noted that the Sahara, because it has a high albedo, is a net sink of radiation even in the summer (Fig 4.1). According to his simple model, and according to

observations, this overall cooling relative to surrounding areas results in subsidence in the troposphere, with large-scale convergence at the upper levels and divergence in the lower troposphere. Thus convection is suppressed and the desert conditions are perpetuated. Charney therefore, with the support of integrations of an atmospheric general circulation model (AGCM) forced with regional changes of albedo, conjectured that the Sahel drought, then about 7 years old, might have been partly caused or maintained by an extension of this subsidence as a result of an increased albedo of the ground in the Sahel. This increased albedo could have occurred initially through overgrazing by animals, or could have been a result of an initial lack of rainfall.

A possible problem with Charney's idea is that if there is initially considerable cloudiness and precipitation as a result of large-scale convergence, then although a small increase in albedo might initiate sinking motion, this would tend to reduce cloud cover. Solar heating would then increase, offsetting the effects of the reduced albedo, and perhaps preventing a further increase in sinking motion.

A more serious problem is that satellite data compiled since Charney formulated his hypothesis do not appear to show a systematic increase of albedo, at least in the western half of the Sahel, since just prior to the commencement of the drought (Fig 4.2). Norton et al (1979) (triangles in Fig 4.2) had found an increase of albedo between 1967 and 1974 in the western half of the Sahel, especially in the wet season, but Courel et al (1984) found a subsequent and stronger decrease,, which may have resulted from accumulation of plant debris in protected areas, or from recovery of grass cover.

Finally, Charney's model took no account of the direct effects of a deficiency of local soil moisture on the heat budget of the atmosphere. We will therefore now consider these effects, before giving an account of some atmospheric general circulation model experiments designed to assess the impact of variations of both soil moisture and albedo. In Lecture 5,

however, we will demonstrate that it is interhemispheric patterns of sea surface temperature change which appear to have had most impact on Sahel rainfall.

## 4.2 A GENERAL DISCUSSION OF THE EFFECT OF SOIL MOISTURE VARIATIONS ON PRECIPITATION

Why should we think that soil moisture variations could be important to regional precipitation? Evaporation of water from the ground surface is complex but essentially depends on three factors:-

(a) The difference in vapour pressure between the soil surface and a representative level above the soil. The vapour pressure at the soil surface is usually taken as the saturation vapour pressure of water at the temperature of the soil surface: thus evaporation is taken to depend on ground temperature.

(b) The wind speed near the ground.

(c) The availability of soil water, or "soil moisture deficit".

A simple version of Penman's climatological evaporation formula (Penman (1956)) expresses the first two factors:-

$$E_p = 0.36\ (e_s - e_a)\ (0.5 + 0.54v)$$

where $e_s$ is the saturation vapour pressure (mb) at the prevailing surface temperature, $e_a$ is the average average vapour pressure of the air (mb), and v is the average wind speed (m/sec) at a height of 2 m.

$E_p$ is known as the potential evaporation and is nominally the actual evaporation over a flat, fresh-water, surface. However the actual evaporation from a ground surface, E', is often less than $E_p$ when S, the soil water content, falls below a certain value. Thus a resistance to evaporation builds up as the surface soil layers dry out and the soil water is evaporated from deeper layers. In some AGCM's E' is parameterised as:-

$$E' = \frac{E_p S}{KS_0}$$

where S is the soil water content, ie the equivalent depth of water existing in the soil, $S_0$ is the maximum water content of the soil, or its "field capacity" and K is a constant; $\frac{E_p}{KS_0}$ is sometimes called ß.

This formula is a gross oversimplification for vegetated surfaces but does express the most important variations of evaporation rate. For a discussion of evaporation formulae and the water balance of the world, see the authoritative references Baumgartner and Reichel (1975), and Korzun (1978).

### 4.2.1 A schematic demonstration of the importance of soil moisture content to precipitation anomalies

Fig 4.3 shows an idealised picture of the exchange of energy between the ground surface and the atmosphere involving soil moisture and evaporation. Imagine there is no horizontal motion and that cloudiness is fixed. Consider the heat balance of the bottom half of the atmosphere, ie that part below the 500 mb level, and assume that this layer is directly affected by ground surface processes. The heat balance of the atmosphere can be expressed by:-

$$MC_p \frac{dT}{dt} = H + LP - LE \qquad (4.1)$$

where E is the evaporation rate, P is the precipitation rate, H is the sensible heating rate, M is the mass per unit area of the atmosphere between the surface and 500 mb, $C_p$ is the specific heat of air and L is the latent heat of vaporisation. In AGCM's, and the real atmosphere, precipitation tends to depend on a relative humidity of almost 100% being reached at some level. Thus the rate of change of relative humidity r of an air mass moving over an evaporating land surface is a crude measure of

the time it will take for precipitation to form when convection is important. The rate of change of relative humidity will depend on the soil moisture. We can explore this as follows:-

We can write $$\frac{dr}{dt} = \frac{d}{dt}\left[\frac{Q}{Q_s}\right]$$

where

Q is the specific humidity integrated through the column of atmosphere between the surface and 500 mb, above which level moisture content is small;

$Q_s$ is the saturation specific humidity in the same column.

Thus $$\frac{dr}{dt} = \frac{1}{Q_s}\frac{dQ}{dt} - \frac{Q}{Q_s^2}\frac{dQ_s}{dt} \qquad (4.2)$$

Now $\frac{dQ}{dt} = E - P$ by definition;

Furthermore $\frac{dQ_s}{dt} \simeq \frac{\delta Q_s}{\delta T}\frac{dT}{dt}$ ,

$\frac{\delta Q_s}{\delta T} \simeq cQ_s$ where c is a constant, and $Q = rQ_s$.

So $$\frac{dr}{dt} = \frac{E-P}{Q_s} - c\,r\frac{dT}{dt}$$

From equation (4.1)

$$\frac{dT}{dt} = \frac{1}{MC_p}\left[H + L(P - E)\right]$$

We can put H + LE = K, a constant, if the total net rate of heating of the ground due to fixed incident radiation remains constant even though the rate of evaporation may vary due to a reduction in soil moisture. It is easily found that

$$\frac{dr}{dt} = (E - P) \left[ \frac{1}{Q_s} + \frac{2cLr}{MC_p} \right] - \frac{cr}{MCp} (K-LP)$$

$$\frac{dr}{dt} = (E - P) \left[ \frac{1}{Q_s} + \frac{2cLr}{MC_p} \right] - \frac{crK}{MC_p} \text{ if P is small (LP<<K).}$$

The total net heating rate in reasonably sunny conditions in June in S England is approximately the equivalent of 5 mm of evaporation each day, ie $K/L$ is about 0.5 g day $^{-1}$ cm$^{-2}$. Now c $\simeq$ 0.07°K$^{-1}$ from tables or the Clausius-Clapeyron equation; L = 2500 Jg$^{-1}$; $MC_p$ = 500 J cm$^{-2}$ °K$^{-1}$ for a 500 mb depth of atmosphere; $Q_s$ is typically about 3 gm cm$^{-2}$ for the lowest 500 mb. Thus,

if $r = \frac{Q}{Q_s} = 0.75$ then $\frac{dr}{dt} \simeq 0.86 (E-P) - 0.135$ day$^{-1}$.

If E = 3 mm/day ie 0.3 gm cm$^{-2}$ day$^{-1}$ and P = 0, then $\frac{dr}{dt} \simeq 0.12$ day$^{-1}$

ie relative humidity increases by 12% per day. If E were 1 mm per day in drought conditions, ie where evaporation is much below the "potential rate", then, still assuming that K remains the same and that P = 0:-

$\frac{dr}{dt} \simeq -5\%$ day$^{-1}$.

In reality, K might be reduced as a result of increased albedo, but even a change as large as 25%, which is not supported by Fig 4.2 for the Sahel, would still yield $\frac{dr}{dt} = -1.5\%$ per day if E were 1 mm per day. So the likelihood of precipitation is much increased by a wet ground surface and decreased by a dry one. In fact most of the evaporation into a mass of air occurs by day, and thus E reaches twice the values indicated above for part

of the day; consequently an air mass need only remain over a soil moisture anomaly for about 12 hours for its relative humidity to be affected by the amount calculated. With typical advecting winds of 10 $ms^{-1}$, the horizontal scale of the soil moisture anomaly need only be about 400-500 km to appreciably affect the humidity of an air-mass moving over it.

## 4.3 EXAMPLES OF THE SENSITIVITY OF CLIMATE TO ALBEDO ($\alpha$) AND S AS SHOWN BY AGCM EXPERIMENTS

Mintz (1984) provides a very good summary of 11 AGCM experiments. Some of these are among the examples below, which are chosen to elucidate the problems.

### 4.3.1 Experiments with $\alpha$ fixed and different anomaly and control S

(From Shukla and Mintz (1982))

This experiment used the global AGCM of the NASA Goddard Space Flight Center's Laboratory for Atmospheric Sciences (GLAS).

(a) Control - land-surface evaporation was everywhere set at the potential rate $E_p$ i.e. $\beta$ was always 1 where $E = \beta E_p$. So the soil was wet everywhere. Albedo varied according to a standard climatology. Initial conditions were for 15 June of a specific year.

(b) Anomaly - no evaporation was allowed anywhere, i.e. the soil was completely dry. Otherwise initial conditions were identical.

The results shown are averages for the following "July". Fig 4.4 shows the precipitation fields for both anomaly and control, Fig 4.5 shows the ground surface temperatures and Fig 4.6 the MSL pressure fields.

Precipitation was greatly reduced over the continents in the anomaly experiment, except over northern South America and in part of Southern Asia. Sahel rainfall, which is a product of the intertropical convergence

zone (ITCZ), was reduced in this experiment. Furthermore, in the anomaly experiment, there was some reduction of overall precipitation over the oceans.

The most dramatic effect of stopping evaporation over land was to greatly increase the surface temperature of the ground in the summer half of the world and in the tropics. Part of this increase in temperature resulted from decreased cloudiness as is shown by the increase of $R_s$, the solar heating rate, in Fig 4.7. The ground also warmed because there was less evaporative cooling (Fig 4.7). Not surprisingly, long-wave radiation losses from the ground were larger and the sensible heating of the air by the ground increased. Above-normal surface air temperatures have been observed in the Sahel and surrounding regions during the drought (Fig 4.8). These warmings, though of up to 3°C, are not as large as the ground temperature increases simulated by Shukla and Mintz, because the changes in evaporation in their experiment were unrealistically large and because ground temperature is even more sensitive to surface heat exchanges than is air temperature.

Fig 4.6 shows that, on the whole, pressure fell over the continents and rose over the oceans in Shukla and Mintz's anomaly experiment, giving a strong global monsoon circulation component to the anomalous atmospheric response. No estimates of statistical significance were given but a qualitative response of the kind shown is physically reasonable and was shown in other similar AGCM experiments e.g, those designed to simulate changes in the latitudinal distribution of solar radiation (Lecture 8).

### 4.3.2 Different values of $\alpha$ but fixed values of S

(Charney et al (1977))

Here we look at a restricted but interesting aspect of Charney et al's results; the Sahel drought is a theme of these lectures, so we will look at the energy balance over the Sahel when $\alpha$ is changed.

(a) Control - where the continents are ice and snow free they were given an albedo of 0.14 though where true deserts are observed, the albedo was set to 0.35 (Fig 4.9).

(b) Anomaly - conditions were the same except that the albedo was increased from 0.14 to 0.35 in the "Sahel", in Rajputana (India) and also in the Western Great Plains (USA), all adjacent to true deserts (see Fig 4.9). Table 4.1 shows detailed results for the energy balance of the Sahel which are instructive, given Charney's original paper of 1975. The main points are:

(i) The evaporation rate, $\beta E_p$, was fixed at 0.51 $E_p$ in both experiments.

(ii) The rate of solar heating of the ground, $R_s$, increased slightly as $\alpha$ increased; this paradoxical result arose because the model cloudiness, N, decreased greatly from 0.7 to 0.46, more than was necessary to offset the effects of an increased value of $\alpha$.

(iii) Evaporation E decreased in the anomaly experiment, though only by 1 mm/day.

(iv) Sensible heating H of the atmosphere by the ground increased in the anomaly experiment.

(v) In the anomaly experiment net outgoing long-wave radiation $R_L$ increased because the skies were clearer and the air was less humid.

(vi) Net radiation, $R_N$, became less positive in the anomaly experiment.

(vii) Surface temperature $T_A$ fell in the anomaly experiments but only very slightly.

(viii) The convergence of water vapour in the anomaly experiment decreased very strongly, by the equivalent of 2.5 mm of precipitation per day.

(ix) Precipitation was considerably reduced in the anomaly experiment, by 3.4 mm per day, mostly because of the decreased moisture convergence rather than because of the decreased evaporation.

So the dynamical effect of decreased convergence from more distant locations was dominant when $\alpha$ was increased. But surface temperatures hardly altered, even though the availability of soil moisture was fixed, as effectively assumed in Charney's original model. Such results clearly depend on the model used but show the fascinating complexity of the problem. They do not prove however that an increase in albedo is necessarily the chief (local) cause of the Sahel drought as the next section will suggest.

### 4.3.3 Fixed $\alpha$, but different time-dependent soil moisture variations

(Owen et al (1988))

The AGCM integrations of Owen et al (1988) were designed to assess the impact of observed worldwide sea surface temperature anomalies, and the additional impact of soil moisture feedback, on rainfall in the Sahel. The experiments were carried out with the Meteorological Office 11-layer GCM (Slingo (1985)) which has a resolution of 2.5° latitude by 3.75° longitude. A control integration with climatological sea surface temperatures and interactive soil moisture was used to determine the model's climatology of soil moisture as well as its atmospheric climatology. Then eight anomaly integrations were carried out, using observed worldwide sea surface temperatures for 1950, 1958, 1983 and 1984 respectively, firstly with interactive soil moisture, and secondly with the soil moisture constrained to equal the model's climatological values. Each integration covered approximately the period April to October inclusive. The first two months were intended to allow the model to adjust to the imposed sea surface

temperatures from the identical starting atmospheric conditions, which were those of 26 March 1984. The results for June to October are summarised in Fig 4.10, where (I) and (C) denote interactive and climatological soil moisture respectively. Fig 4.10A includes the observed rainfalls in the Sahel. It is clear that the encouraging ability of the model to simulate the very different rainfalls observed in each of the four years derived largely from the differences in sea surface temperatures (see also Lecture 5). However, soil moisture feedback did have an impact on the results. This is clearly seen in 1950 when the simulated soil moisture was very plentiful (Fig 4.10B) and in 1983 when the simulated soil was very dry, though the inclusion of interactive soil moisture did not systematically either improve or degrade the simulated rainfalls (Fig 4.10A). Owen et al found that the use of interactive as opposed to climatological soil moisture had little effect on the AGCM's atmospheric circulation, despite a substantial impact on surface and lower-tropospheric temperatures over and around the Sahel (Fig 4.11), such that hotter conditions occurred in the dry years, in agreement with observations (Fig 4.8), when interactive soil moisture was used (Fig 4.11A), but not with climatological soil moisture (Fig 4.11B).

### 4.3.4 Simulation of deforestation

(Dickinson and Henderson-Sellers (1988))

We give a brief description of this simulation of the deforestation of the Amazon basin in order to draw attention to a few of the complexities involved. Dickinson and Henderson-Sellers's AGCM anomaly simulation included the following changes to the surface over much of South America between 10°N and 15°S, representing the replacement of broad-leaved evergreen forest by scrub-grassland:

| | |
|---|---|
| Vegetation cover: | reduced by 10% of land area |
| Roughness length of vegetation: | reduced from 2 m to 5 cm |
| Vegetation albedo at wavelengths | |

| | | |
|---|---|---|
| | $< 0.7$ μm: | increased from 0.04 to 0.08 |
| | $\geq 0.7$ μm: | increased from 0.20 to 0.30 |
| Dry soil albedo at wavelengths | | |
| | $< 0.7$ μm: | increased by 0.04 |
| | $\geq 0.7$ μm: | increased by 0.08 |
| Saturated soil albedo at wavelengths: | | |
| | $< 0.7$ μm: | increased by 0.02 |
| | $\geq 0.7$ μm: | increased by 0.04 |
| Soil depth: | | reduced from 1.5 m to 1 m |
| Runoff: | | formulation modified so that runoff decreased less rapidly with drying of the surface layer. |

Dickinson and Henderson-Sellers' AGCM control and anomaly integrations of 13 months were too short for statistically significant changes in local rainfall, or non-local climatic effects, to be confirmed. Over the deforested area, however, surface air temperatures were systematically higher in the anomaly run by an average of nearly 2°C, and soil surface temperatures were raised by an average of over 3°C. Total evaporation decreased by an average of about 0.5 mm per day. Total soil moisture decreased by up to 20 cm but this change was a result of the specified reduced depth of soil: the soil actually became a little more saturated. Interception of precipitation by the vegetation canopy was decreased by an average of about 0.4 mm per day: intercepted precipitation is re-evaporated in the model. Dickinson and Henderson-Sellers interpreted their AGCM results in terms of the effects on a land-surface model, with prescribed

atmospheric conditions, of the various changes to the surface layer accompanying deforestation, and concluded that the reduction in the vegetation roughness length had the largest overall effect on the thermodynamics of the surface.

## 4.4 CONCLUSION

The results presented in this section suggest that correct treatments of soil moisture and albedo will contribute limited increases of predictability on monthly, seasonal and interannual time-scales. In forested areas other features such as vegetation-induced roughness are also likely to be important, but their non-local effects have yet to be demonstrated. By contrast, we show in the next lecture that interactions between the atmosphere and the sea surface have major implications on a worldwide scale.

We are grateful to Dr P Rowntree for the basis of Section 4.2.1.

TABLE 4.1 COMPONENTS OF THE ENERGY AND WATER BUDGETS, IN EXPERIMENT OF CHARNEY ET AL (1977)

| Region | Case No | (1) β | (2) (1-A) | (3) $R_S$ | (4) $R_L$ | (5) $R_N$ | (6) LE | (7) H | (8) N | (9) $T_A$ | (10) E | (11) (-∇.qv) | (12) P |
|---|---|---|---|---|---|---|---|---|---|---|---|---|---|
| Sahel | 2a (Control) | 0.51 | 0.86 | 169 | 58 | 111 | 107 | 4 | 0.70 | 26.0 | 3.7 | 3.7 | 7.4 |
| (16°-20°N 17.5°W-37.5°E | 3a (Anomaly) | 0.51 | 0.65 | 177 | 84 | 93 | 81 | 12 | 0.46 | 25.7 | 2.8 | 1.2 | 4.0 |

KEY

β: ratio of actual to potential evaporation rates

α: albedo

$R_S$: rate of solar heating of the ground ($Wm^{-2}$)

$R_L$: net longwave radiation from the ground ($Wm^{-2}$)

$R_N$: rate of net radiative heating of the ground = $R_S - R_L$ ($Wm^{-2}$)

LE: rate of latent heat transfer from the ground to the atmosphere ($Wm^{-2}$)

H: rate of sensible heat transfer from the ground to the atmosphere ($Wm^{-2}$)

N: cloudiness fraction

$T_A$: surface temperature (°C)

E: evaporation rate (mm/day)

$-\nabla.qv$: convergence of water vapour (mm/day)

P: precipitation (mm/day)

## REFERENCES TO LECTURE 4


BAUMGARTNER A and REICHEL E (1975) The World Water Balance: Mean annual global, continental and maritime precipitation, evaporation and run-off. Elsevier.

CHARNEY, J G (1975) Dynamics of deserts and drought in the Sahel. Q J Roy Met Soc, 101, 193-202.

CHARNEY J, QUIRK W J, CHOW S-H AND KORNFIELD J (1977) A comparative study of the effects of albedo change and drought in semi-arid regions. J Atmos Sci, 34, 1366-1385.

COUREL, M F, KANDEL, R S and RASOOL, S I (1984) Surface albedo and the Sahel drought. Nature, 307, 528-531.

DICKINSON, R E and HENDERSON-SELLERS, A (1988) Modelling tropical deforestation: a study of GCM land-surface parametrizations. Q.J.R Meteorol. Soc., 114, 439-462.

KORZUN V I (Ed) (1978) World Water balance and water resources of Earth. Studies and Reports in Hydrology, Vol 25, Unesco Press, Paris.

MINTZ Y (1984) The sensitivity of numerically simulated climates to land-surface boundary conditions. The Global Climate, pp 79-105. Ed: J T Houghton, Cambridge University Press.

NORTON, C C, MOSHER, F R and HINTON, B (1979) An investigation of surface albedo variations during the recent Sahel drought. J. Appl. Met., 18, 1252-1262.

OWEN, J A, FOLLAND, C K and BOTTOMLEY, M (1988) Numerical simulation of seasonal Sahel rainfall in four past years using observed sea surface temperatures. Long Range Forecasting and Climate Research Memo No 15, Meteorological Office, Bracknell.

PENMAN H L (1956) Estimating Evaporation. Trans Amer Geophys Union, 37(1), 43-46.

SHUKLA J AND MINTZ Y (1982) Influence of land-surface evapotranspiration on the earth's climate. Science, 215, 1498-1501. Also presented at the Joint Scientific Committee Study Conference on Land Surface Processes in Atmospheric General Circulation Models, Greenbelt, USA, 5-10 January 1981 (this is reference on diagrams).

SLINGO, A (1985) Handbook of the Meteorological Office 11-layer atmospheric general circulation model. Dynamical climatology Tech Note No 29, Meteorological Office, Bracknell.

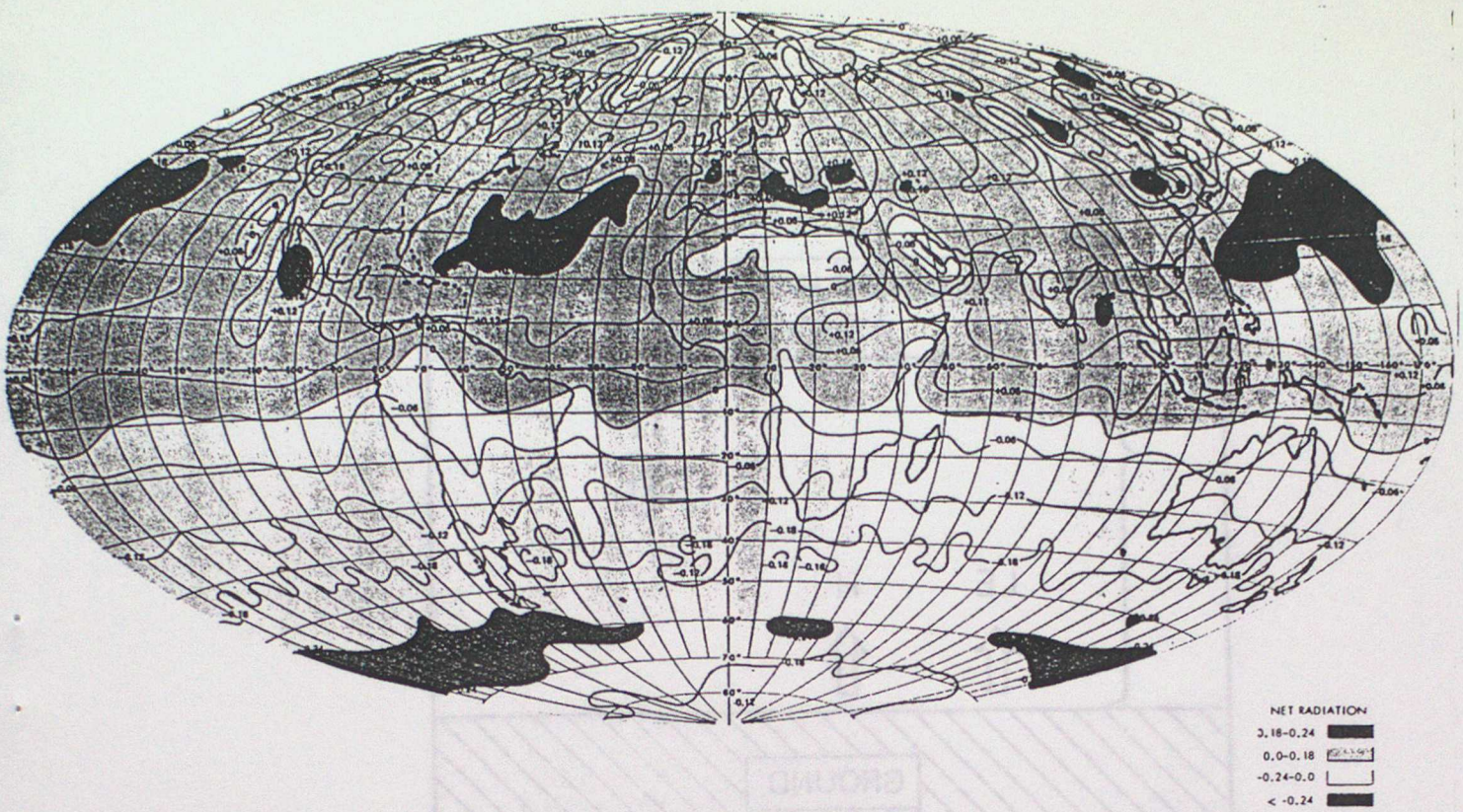


Net radiation at the top of the atmosphere (cal/cm²/min) measured from Nimbus III, 1–15 July 1969.
Multiply by 697 to give $Wm^{-2}$.

Figure 4.1. From Charney (1975).

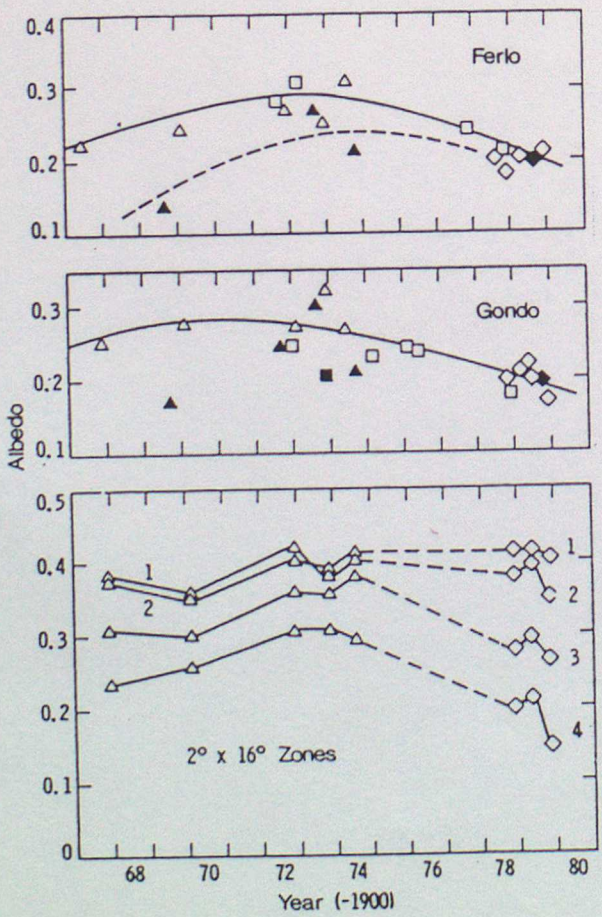


Figure 4.2.

Albedo history of the western Sahara and Sahel between 1967 and 1979. Triangles, estimates based on the 2° maps of Norton et al (1979); squares, Landsat data for Ferlo (15-17N, $13\frac{1}{2}$-$15\frac{1}{2}$W) and Gondo ($13\frac{1}{2}$-15N, $2\frac{1}{2}$-$4\frac{1}{2}$W); lozenges, Meteosat-1 data. The filled symbols correspond to observations in the rainy season. Curves 1-4 are integrated albedo values for the strips 22-20N, 20-18N, 18-16N, 16-14N extending from 16W to the Greenwich meridian.

After Courel et al (1984).

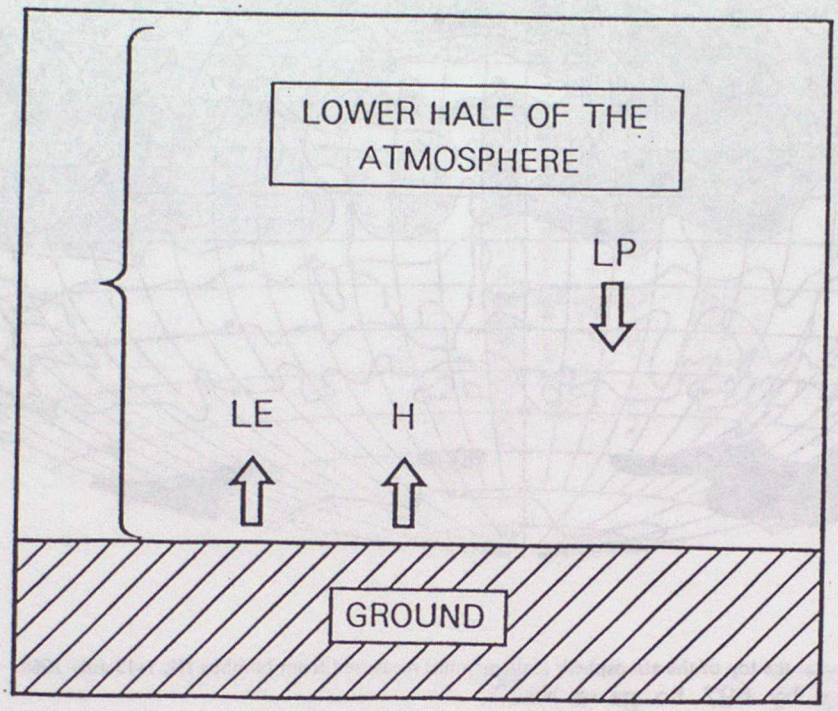


Figure 4.3. Schematic of exchanges of latent and sensible heat at the surface.

Precipitation (mm/day) in wet-soil case (top) and dry-soil case (bottom), in experiment of Shukla & Mintz (1981). (Precipitation greater than 2 mm/day is shaded.)

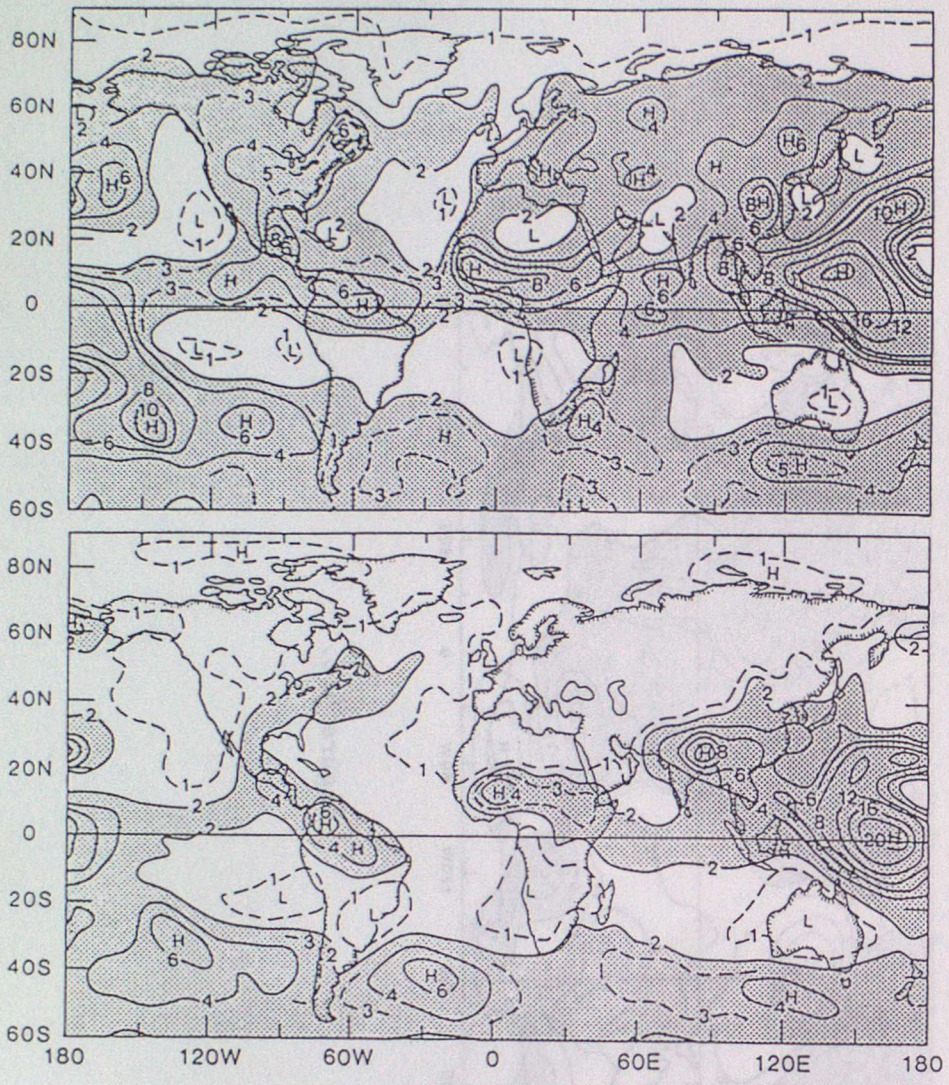


Figure 4.4.

Ground-surface temperature (°C) in wet-soil case (top) and dry-soil case (bottom), in experiment of Shukla & Mintz (1981).

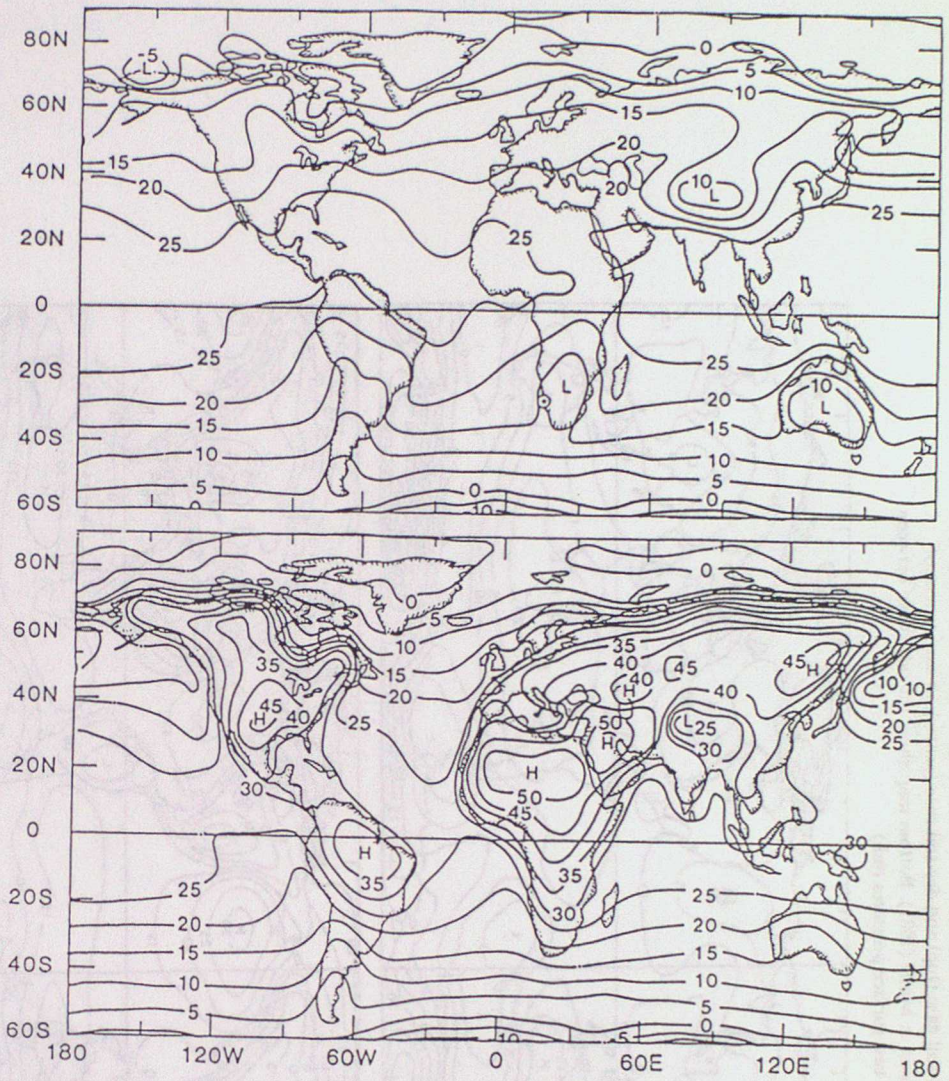


Figure 4.5.

Surface pressure reduced to sea level (mb minus 1000) in wet-soil case (top) and dry-soil case (center), in experiment of Shukla & Mintz (1981). Bottom map show the difference between the two surface pressures (mb).

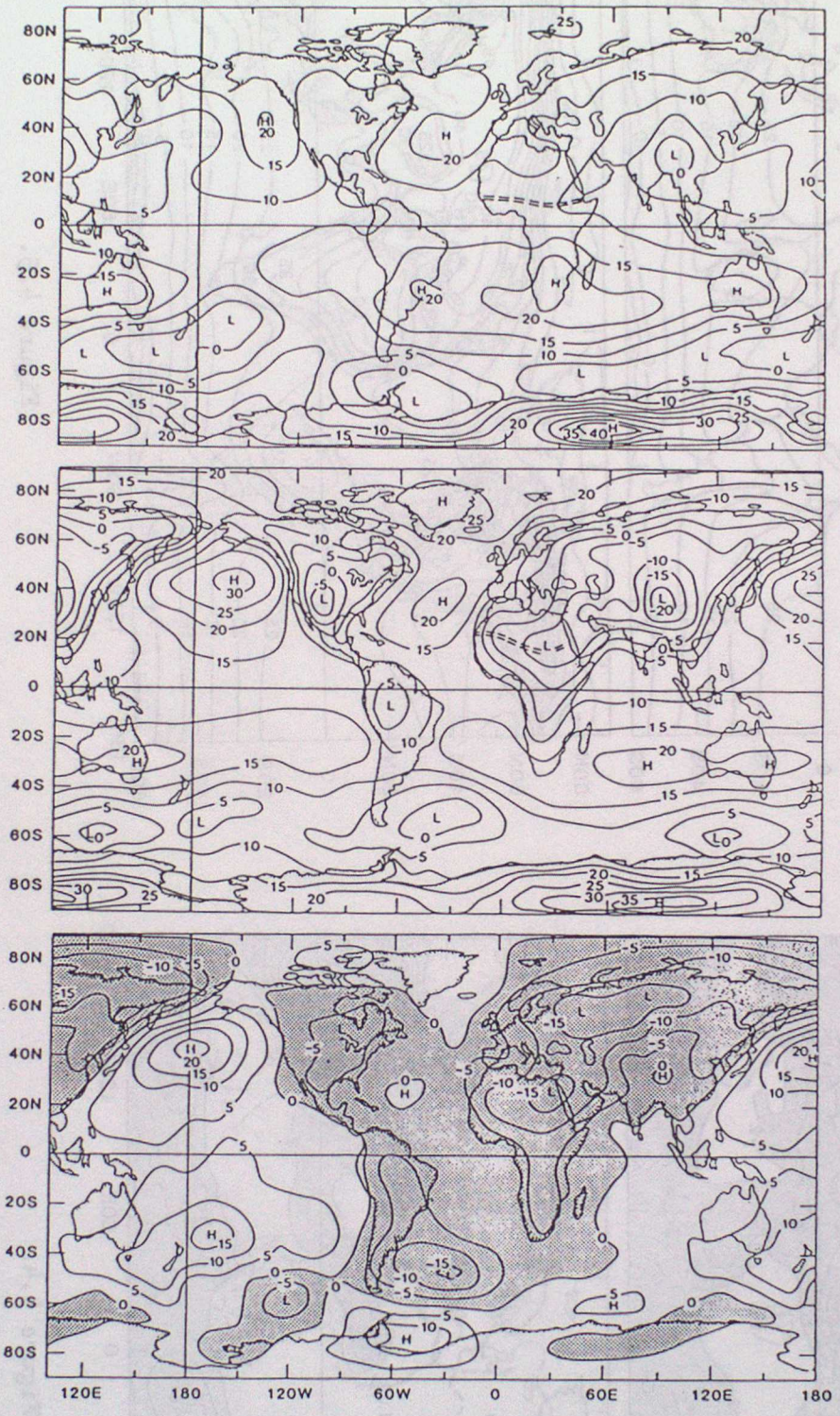


Figure 4.6.

Surface energy transfers (watt/m²) averaged for the continents between 20°S and 60°N, in experiment of Shukla and Mintz (1981).

$R_S$ solar raditional heating of the ground.

$R_L$ long wave radiational cooling of the ground (difference between radiation emitted by ground and radiation absorbed by ground).

$R_N = (R_S - R_L)$ net (all-wavelength) radiational heating of the ground.

$LE$ latent heat transfer from ground to atmosphere (evaporative cooling of the ground).

$H$ conductive-convective heat transfer from ground to atmosphere.

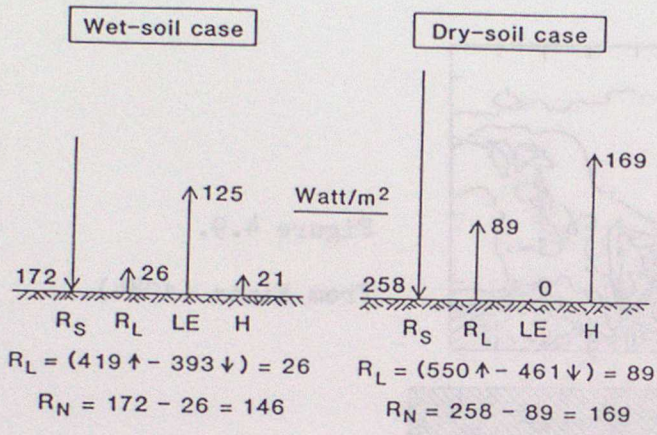


Figure 4.7.

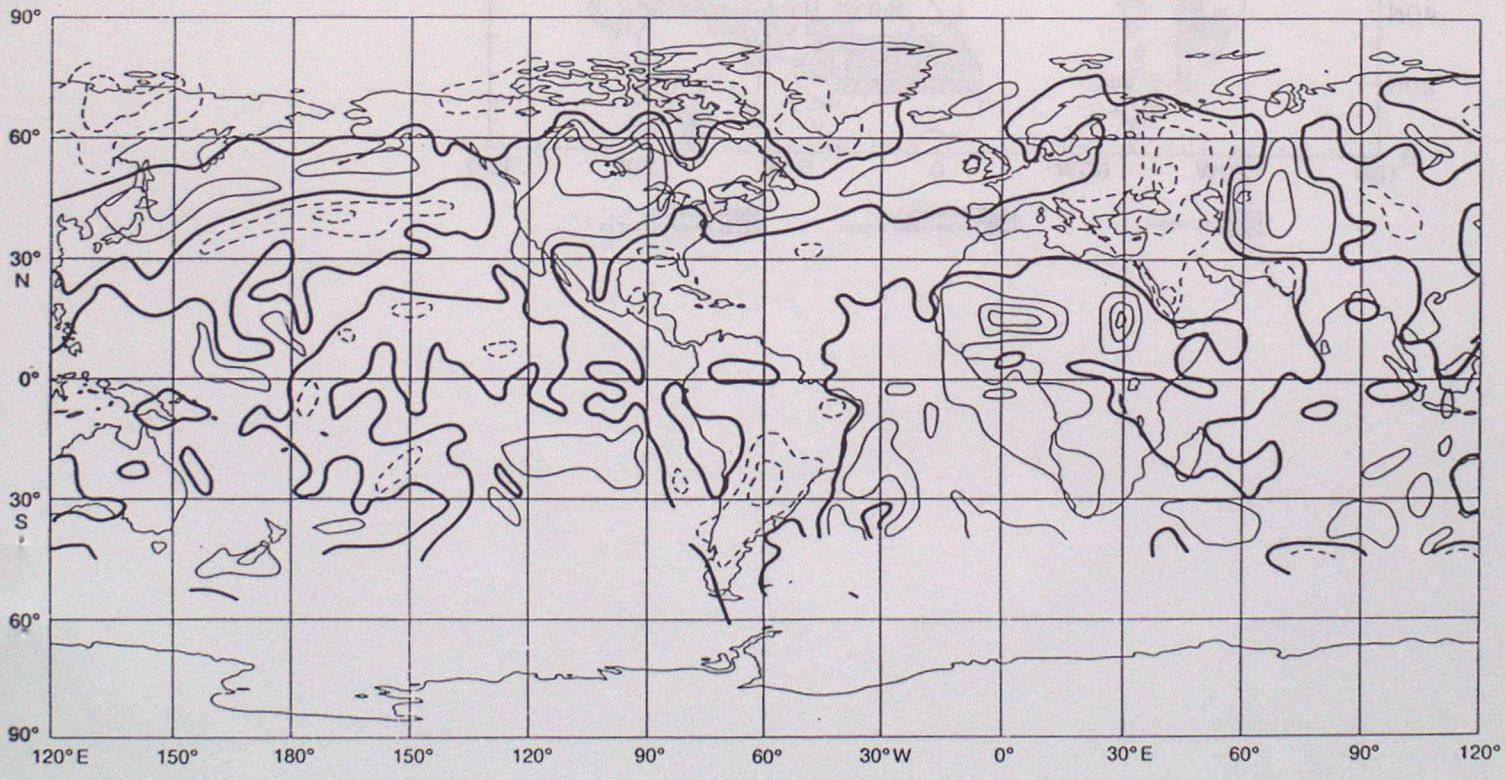


Figure 4.8. Sea surface temperature and land air temperature (w.r.t.1951-80), August 1984. Contours every 1°C (Light solid, positive; heavy solid, zero; dashed, negative). Values over land from P.D.Jones (Univ. East Anglia).

Bottom panel: the assigned albedos in experiments of Charney *et al.* (1977). Unshaded land areas have an albedo of 0.14 in all cases, and dot-shaded areas have an albedo of 0.35 in all cases. In the cross-ruled areas the albedo was changed from 0.14 (in cases 2a and 2b) to 0.35 (in cases 3a and 3b). Top panel: precipitation (mm/day) in case 3b.

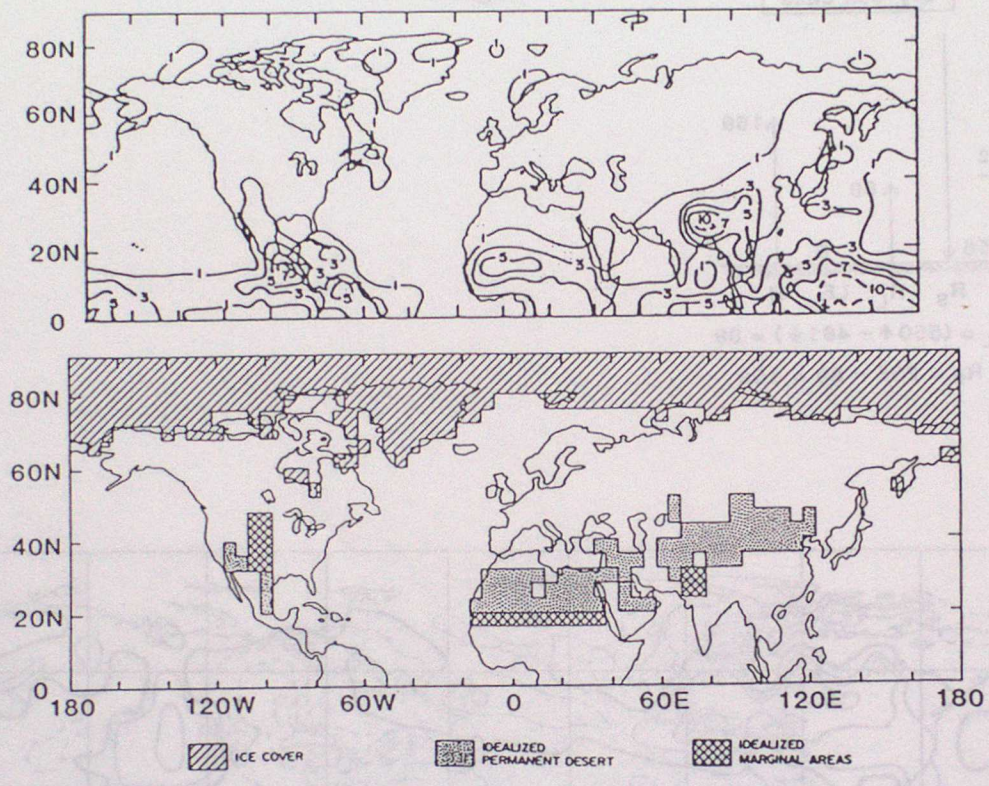


Figure 4.9.

From Mintz (1984).

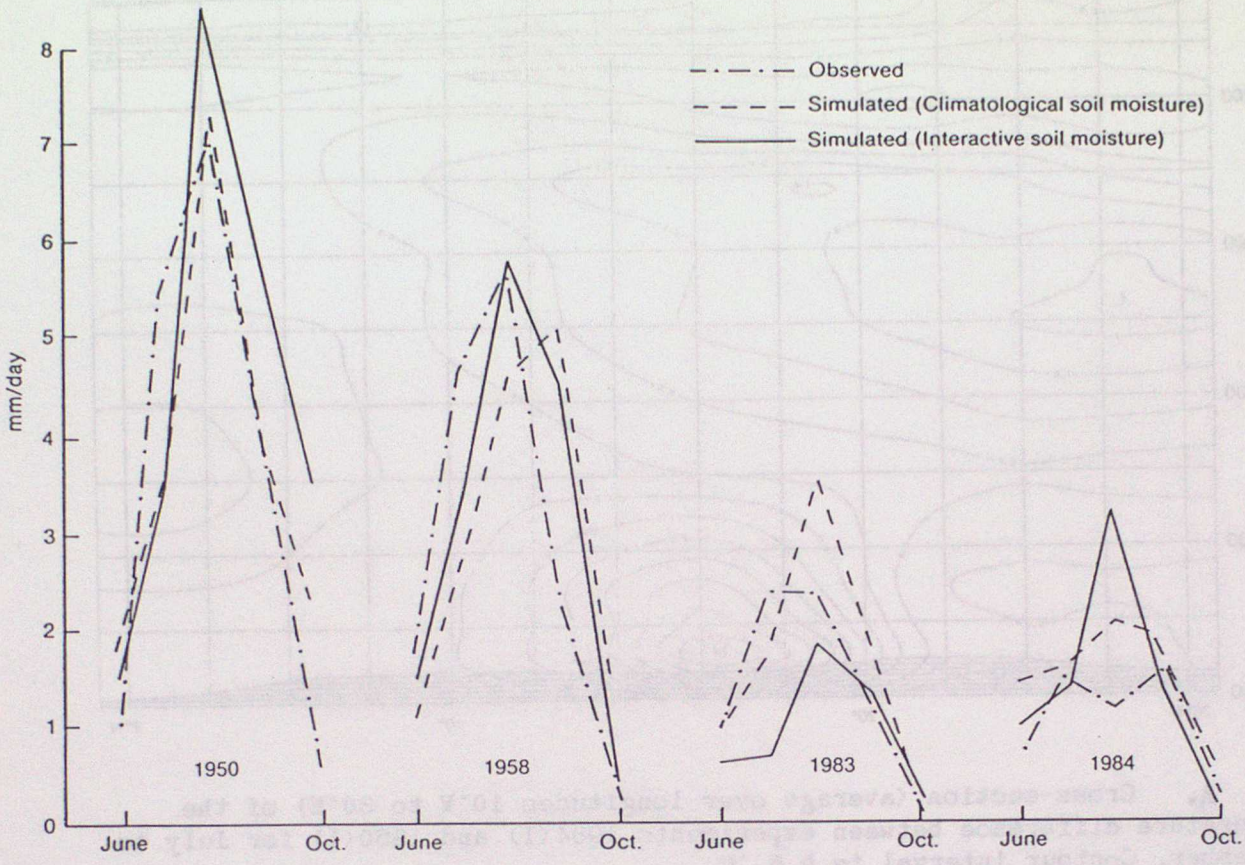


A. Time series of simulated rainfall for the whole Sahel for experiments 1950(I), 1958(I), 1983(I), 1984(I), 1950(C), 1958(C), 1983(C) and 1984(C), together with the corresponding observed rainfall.

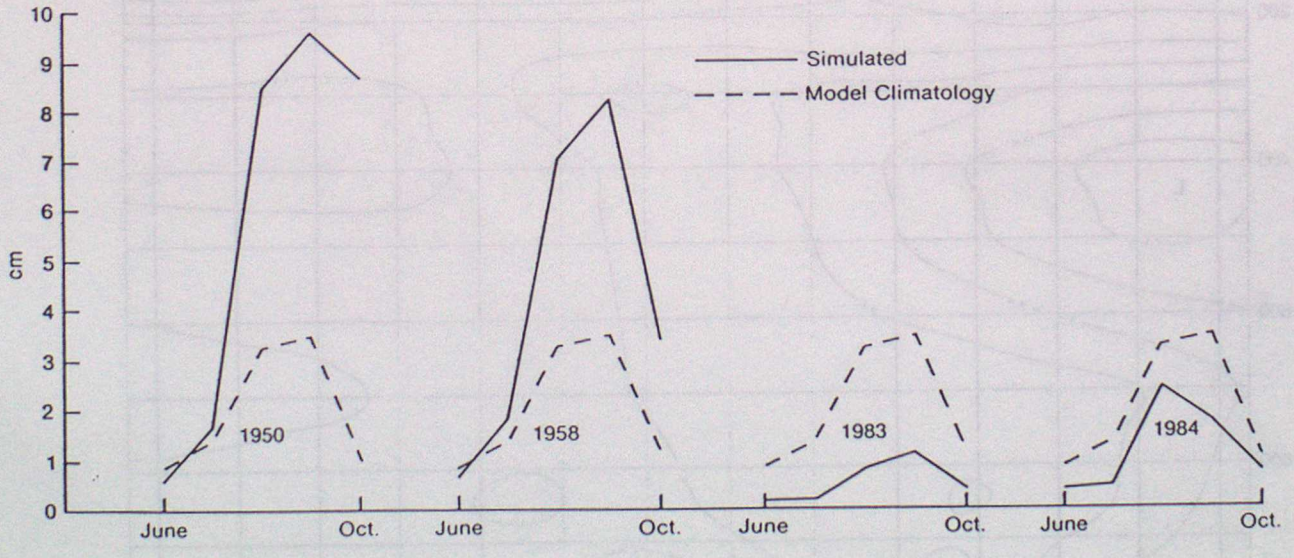


B. Time series of simulated soil moisture for the whole Sahel for experiments 1950(I), 1958(I), 1983(I) and 1984(I).

Figure 4.10. From Owen et al (1988).

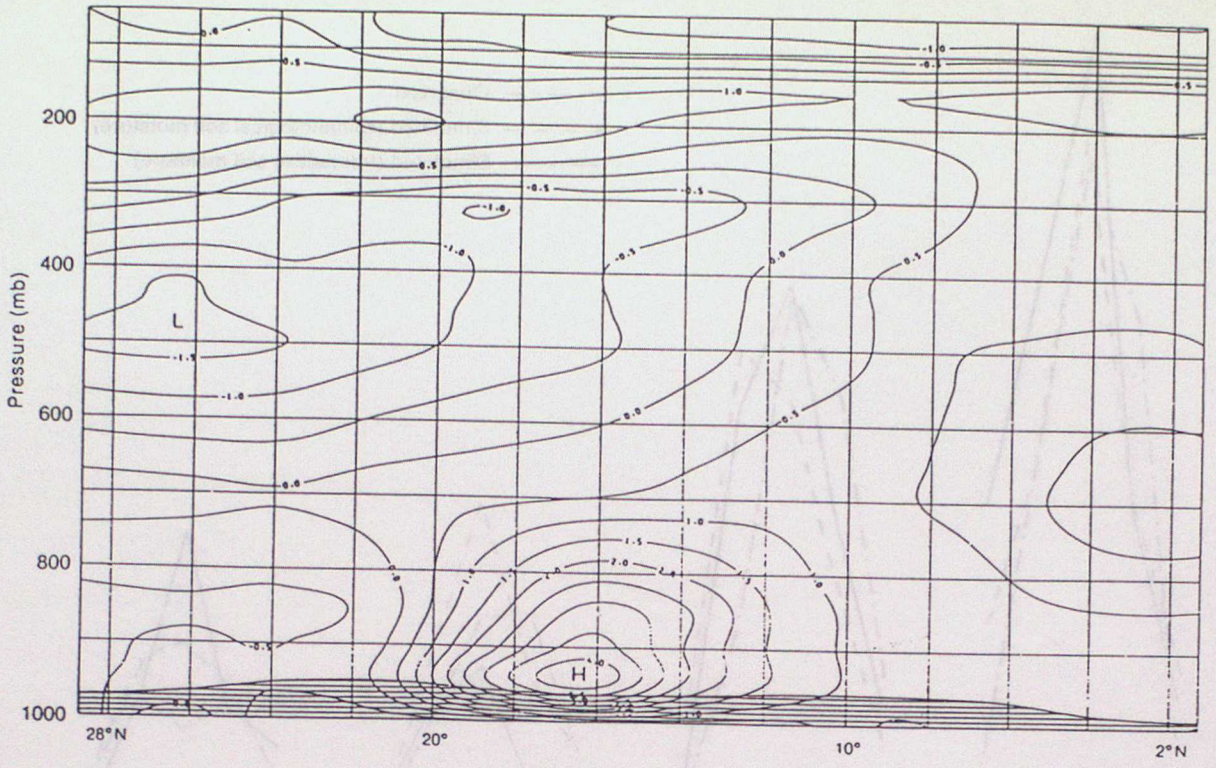


A. Cross-section (average over longitudes 10°W to 30°E) of the temperature difference between experiments 1984(I) and 1950(I) for July to September. Contour interval is 0.5 °C.

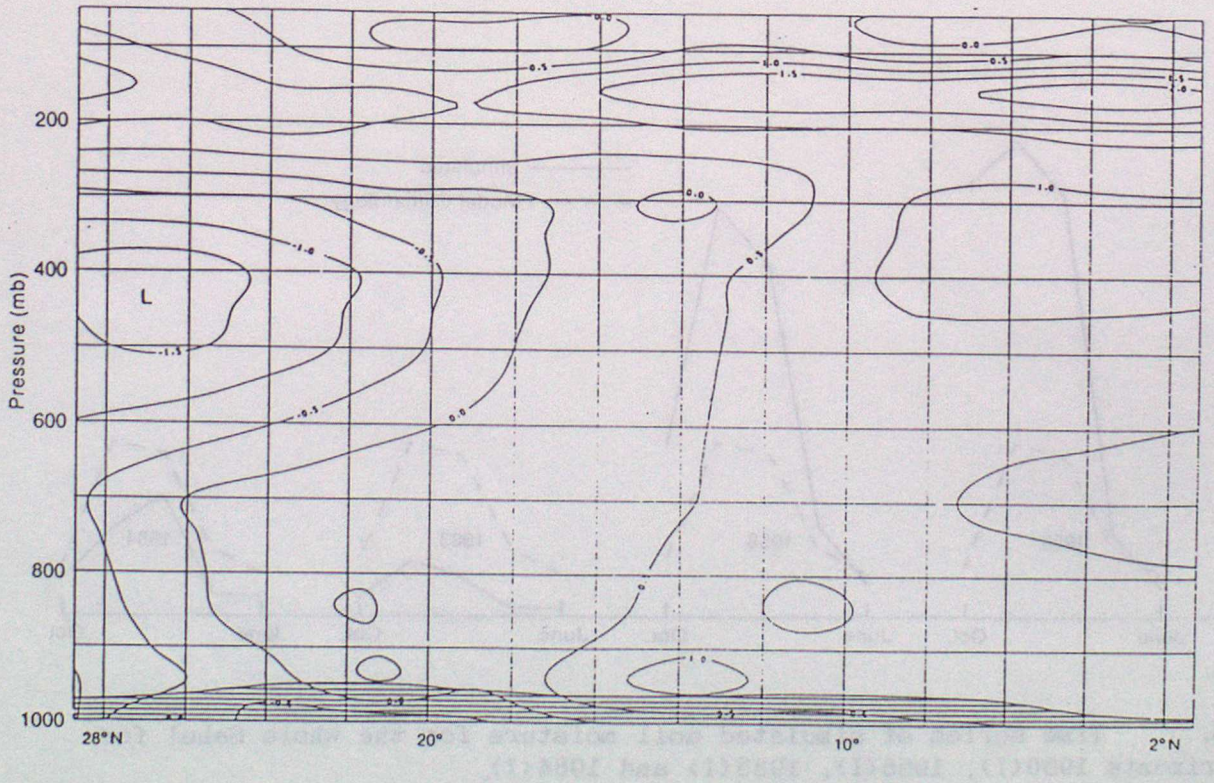


B. As A but for experiments 1984 (C) and 1950 (C).

Figure 4.11. From Owen et al (1988).

INDEX TO LONG-RANGE FORECASTING AND CLIMATE RESEARCH SERIES

1) THE CLIMATE OF THE WORLD - Introduction and description of world climate.
by C K Folland (March 1986)

2) THE CLIMATE OF THE WORLD - Forcing and feedback processess.
by C K Folland (March 1986)

3) THE CLIMATE OF THE WORLD - El Nino/Southern Oscillation and the Quasi-biennial Oscillation.
by C K Folland (March 1986)

4) THE CLIMATE OF THE WORLD - Climate change: the ancient earth to the 'Little Ice Age'.
by C K Folland

5) THE CLIMATE OF THE WORLD - Climate change: the instumental period.
by C K Folland (March 1986)

6) THE CLIMATE OF THE WORLD - Carbon dioxide and climate (with appendix on simple climate models).
by C K Folland (March 1986)

7a) Sahel rainfall, Northern Hempishere circulation anomalies and worldwide sea temperature changes, (To be published in the Proceedings of the "Pontifical Academy of Sciences Study Week", Vatican, 23-27 September 1986).
by C K Folland, D E Parker, M N Ward and A W Colman (September 1986) (Amended July 1987)

8) Lagged-average forecast experiments with a 5-level general circulation model.
by J M Murphy (March 1986)

9) Statistical Aspects of Ensemble Forecasts.
by J M Murphy (July 1986)

10) The impact of El Nino on an Ensemble of Extended-Range Forecasts. (Submitted to Monthly Weather Review)
by J A Owen and T N Palmer (December 1986)

11) An experimental forecast of the 1987 rainfall in the Northern Nordeste region of Brazil.
by M N Ward, S Brooks and C K Folland (March 1987)

12) The sensitivity of Estimates of Trends of Global and Hemispheric Marine Temperature to Limitations in Geographical Coverage.
by D E Parker (April 1987)

13) General circulation model simulations using cloud distributions from the GAPOD satellite data archive and other sources.
by R Swinbank (May 1987)

14) Similation of the Madden and Julian Oscillation in GCM Experiments.
by R Swinbank (May 1987)

15) Numerical simulation of seasonal Sahel rainfall in four past years using observed sea surface temperatures.
by J A Owen, C K Folland and M Bottomley (April 1988)

16) Not used

17) A note on the use of Voluntary Observing Fleet Data to estimate air-sea fluxes.
by D E Parker (April 1988)

18) Extended-range prediction experiments using an 11-level GCM
by J M Murphy and A Dickinson (April 1988)

19) Numerical models of the Raingauge Exposure problems - field experiments and an improved collector design.
by C K Folland (May 1988)

20) An interim analysis of the leading covariance eigenvectors of worldwide sea surface temperature anomalies for 1901-80.
by C K Folland and A Colman (April 1988)

21) Prospects for long range forecasting for the United Kingdom.
by A Dickinson and C K Folland (July 1988)

22) CLIMATE OF THE WORLD (Restricted Issue) 1. Introduction to world climate

2. Description of world climate
by C K Folland and D E Parker (July 1988)

23) CLIMATE OF THE WORLD (Restricted issue) 3. Climatic forcing and feedback processes.
I. Forcing from above.

4. Climatic forcing and feedback processes.
II. Interactions with land surface
by C K Folland and D E Parker (July 1988)

24) CLIMATE OF THE WORLD (Restricted Issue) 5. Ocean-atmosphere interaction
by D E Parker and C K Folland (July 1988)

25) CLIMATE OF THE WORLD (Restricted Issue) 6. The El Nino/Southern Oscillation, the Quasi-Biennial Oscillation, and the 30-60 day variations.
by C K Folland and D E Parker (July 1988)

26) CLIMATE OF THE WORLD (Restricted Issue) 7. A review of palaeoclimate from the early Earth to the Pleistocene ice ages

8. Climate from the late glacial to the "Little ice age"
by C K Folland and D E Parker (July 1988)

27) CLIMATE OF THE WORLD 9. Climatic change in the instrumental period
(Restricted Issue) by D E Parker and C K Folland (July 1988)

28) CLIMATE OF THE WORLD 10. Carbon dioxide and other greenhouse gases, and
(Restricted Issue) climatic variation
(with appendix on simple climate models).
by D E Parker, C K Folland and D J Carson
(July 1988)